Full title:

Modulation of fatty acid elongation sustains sexually dimorphic hydrocarbons and female attractiveness in *Blattella germanica* (L.)

Short title:

Generation and biological significance of sexually dimorphic hydrocarbons

Xiao-Jin Pei [a], Yong-Liang Fan [a, *], Yu Bai [b], Tian-Tian Bai [a], Coby Schal [c], Zhan-Feng Zhang [a], Nan Chen [b], Sheng Li [b], and Tong-Xian Liu [a, *]

[a] State Key Laboratory of Crop Stress Biology for Arid Areas and Key Laboratory of Integrated Pest Management on Crops in Northwestern Loess Plateau, Ministry of Agriculture, Northwest A&F University, Yangling, Shaanxi 712100, P. R. China

[b] Guangdong Provincial Key Laboratory of Insect Developmental Biology and Applied Technology and Institute of Insect Science and Technology, School of Life Sciences, South China Normal University, Guangzhou 510631, China

[c] North Carolina State University, Department of Entomology and Plant Pathology and W.M. Keck Center for Behavioral Biology, Raleigh, North Carolina, USA.

* Corresponding authors:

Y.-L. Fan (yfan@nwafu.edu.cn) and T.-X. Liu (txliu@nwafu.edu.cn).

Abstract

Insect cuticular hydrocarbons (CHCs) serve as important intersexual signaling chemicals and generally show variation between the sexes, but little is known about the generation of sexually dimorphic hydrocarbons (SDHCs) in insects. Here, we report the molecular mechanism and biological significance that underling the generation of SDHC in the German cockroach, *Blattella germanica*. Sexually mature females possess more C29 cuticular hydrocarbons (CHCs), especially the contact sex pheromone precursor 3,11-DimeC29. RNAi screen against fatty acid elongase gene family members and combined with heterologous expression revealed that both *BgElo12* and *BgElo24* were involved in HC production, but *BgElo24* is of wide catalytic activities and is able to provides substrates for *BgElo12*, and only the female-enriched *BgElo12* was responsible for sustaining female-specific HC profile. Repressing *BgElo12* masculinized the female CHC profile, decreased contact sex pheromone level and consequently reduced the sexual attractiveness of female cockroaches. Moreover, the asymmetric expression of *BgElo12* between the sexes is modulated by sex differentiation cascade. Specifically, male-specific *BgDsx* represses the transcription of *BgElo12* in males, while *BgTra* is able to remove this effect in females. Our study reveals a novel molecular mechanism responsible for the formation of SDHCs, and also provide evidences on shaping of the SDHCs by sexual selection, as females use them to generate high levels of contact sex pheromone.

Introduction

Sexual dimorphism is prevalent in the animal kingdom. Females and males independently evolve some traits that enhance survival and reproduction under the pressure of divergent selection forces, thus leading to sexual dimorphism of traits such as body size [1]. Under sexual selection, asymmetric selection on the sexes can also result in the evolution of sexually dimorphic traits; however, these traits are subject to both inter- and intra-sexual selection [2,3]. Because males and females of the same species share the majority of their genomes, the genetic basis of sex-specific traits that evolve under sexual selection is poorly understood. It is widely assumed that sexually dimorphic regulation of gene expression facilitates sex-specific adaptations [4–7]. Recruitment of pre-existing genes or pathways into sexually dimorphic regulatory contexts has been proposed as a remarkable mechanism enabling the divergence of gene expression between the sexes [8–10]. The sex-differentiation pathway is a conserved switch or regulator governing a set of downstream genes that direct sexually dimorphic traits [11,12]. The signaling cascades that transform sex differences (sex-specific chromosomes) into alternative splicing of sex differentiation genes (e.g. *Transformer* and *Doublesex* in insects), and the patterns of splicing these genes into sex-based isoforms have been widely described in different insect orders [13–17]. However, sexually dimorphic traits are usually generated from tightly associated multiple biosynthetic steps that are executed by a series of genes, and the nodes at which sex-determining signals connect with the biosynthetic pathway are poorly understood. Moreover, how these genes are translated into sexually dimorphic traits under elaborate spatial and temporal patterns also needs to be elucidated.

The main function of insect cuticular hydrocarbons (CHCs) is to waterproof the cuticle to resist dehydration under dry conditions [18]. In many insects, CHCs have been coopted to serve as chemical signals (pheromones) that mediate intraspecific communication [19,20]. Sexually dimorphic CHC (SDCHC) profiles are widespread in insects [21–23], but the regulatory networks that underlie the formation of SDCHCs largely remain unknown. Considerable progress has been made toward understanding the genetic basis of HC biosynthesis and CHC variation in insects. An acetyl-CoA carboxylase catalyzes the biosynthesis of malonyl-CoA, and a cytosolic fatty acid synthase (FAS) incorporates malonyl-CoA units onto the acetyl-CoA primer to form linear long-chain fatty acids (LCFAs). A microsomal FAS catalyzes the biosynthesis of methyl-branched LCFAs using methyl malonyl-CoAs [24–30]. The LCF acyl-CoA can be selectively desaturated by a specific fatty acid desaturase (Desat),

68 leading to unsaturated fatty acids [31,32]. The LCF acyl-CoAs are elongated to form very-long-chain fatty
69 acids (VLCFAs) with specific chain lengths by a fatty acid elongation system, including a rate-limiting
70 elongase (ELO) and three other enzymes [29,33]. The VLCF acyl-CoAs are finally reduced to long-chain
71 alcohols by fatty acyl-CoA reductases (FARs) and converted to HCs by the P450 oxidative decarbonylase
72 CYP4Gs [34–36]. It is now clear that the variation in CHCs is primarily reflected in the chain length,
73 number and positions of methyl groups, and the degree of unsaturation, which are determined by ELOs,
74 FASs, and Desats, respectively [37–39]. These genes have been studied in few insect species with regard to
75 SDHCs.

76 In the fruit fly *Drosophila melanogaster*, several studies have elucidated the pheromonal sexual
77 dimorphism of CHCs. Female flies produce C27 and C29 dienes (7,11-heptacosadiene and 7,11-
78 nonacosadiene), both of which function as female-specific contact sex pheromone components, whereas
79 male flies produce C23 and C25 monoenes (7-tricosene and 7-pentacosene) [40]. Ferveur et al. found that
80 the targeted expression of a sex-differentiation gene, *Transformer*, in male oenocytes feminized the male
81 CHC profile, and elicited homosexual courtship from other males [41]. These findings implicated sex-
82 differentiation genes in the production of SDHCs. About 10 years later, Chertemps et al. revealed that the
83 female-specific *desatF* was responsible for the generation of pheromonal dienes in female *D. melanogaster*
84 [31], and they also found that the sexual dimorphism in HC chain length was modulated by the female-
85 specific *eloF* [33]. The specific expression of *desatF* in *D. melanogaster* females was due to a special *cis*-
86 regulatory element (CRE) located upstream of *desatF* in *D. melanogaster*; the CRE presented a doublesex
87 protein (Dsx) binding site that could be recognized by the female-specific isoform of *Dsx* (*Dsx-F*), and the
88 binding of Dsx-F activated the transcription of *desatF*, whereas male-specific Dsx showed no regulatory
89 activity, resulting in sexual dimorphism of *desatF* expression [42]. However, the regulation of other genes
90 involved in the production of SDHCs remains unknown in *D. melanogaster*, and studies in other insects are
91 even rarer.

92 The German cockroach, *Blattella germanica* is a significant worldwide indoor pest [43]. Considerable
93 work has been done on biochemical aspects of CHCs in *B. germanica* [22,44–46]. CHCs in *B. germanica*
94 function as waterproofing agents [47], and as importantly, specific HC components are also the
95 biosynthetic precursors for the production of contact sex pheromone components. 3,11-DimeC29 is the
96 most abundant CHC in females. Its hydroxylation at the 2 position, catalyzed by an age- and sex-specific

putative cytochrome P450 and further oxidation of the -OH generates the main female-specific contact sex pheromone component, 3,11-DimeC29-2-one [48]. The contact sex pheromone is an efficient courtship signal. When a sexually mature male's antennae detect the sex pheromone on the female body surface (mainly the antennae), a "fencing" of male and female antennae ensues. The male then rotates his body and orients the abdominal tip toward the female's head, while raising his wings to expose a specialized tergal gland. Nutrients in the tergal secretion functions as phagostimulants, placing the female in an appropriate position for copulation while she is engaged in feeding on the secretion [49–51]. More recently, Wexler et al. decoded the alternative splicing patterns of sex-differentiation genes in *B. germanica*. BgTra is only functional in females and can splice *BgDsx* into two non-functional female-specific isoforms ($BgDsx^F$), whereas males generate a complete functional male-type *BgDsx* ($BgDsx^M$) [52]. These findings provide opportunities for exploring the mechanisms underlying the SDHCs in *B. germanica*.

In this study, we employed *B. germanica* as a model insect. We characterize the SDCHCs, describe their temporal development, identify *BgElo* genes and provide evidence that *BgElo12* is responsible for the formation of SDCHC profiles. In addition, we found that the female-enriched HCs are important in the generation of the female-specific contact sex pheromone; RNAi of *BgElo12* in females decreased courtship responses of males. Moreover, we show that *BgElo12* is under the regulation of the sex-differentiation pathway; $BgDsx^M$ can specifically repress the transcription of *BgElo12*. These findings suggest that the generation of SDHCs is achieved by placing a fatty acid elongation gene (*BgElo12*) under the regulation of $BgDsx^M$, and linking the sex-differentiation regulatory cascade with the HC biosynthesis pathway, resulting in the asymmetric gene expression and sexually dimorphic HCs in *B. germanica*.

Results

Sexually dimorphic of cuticular hydrocarbons in *B. germanica*

The temporal development of SDCHCs is rarely reported. In order to understand the molecular mechanisms of SDHC generation, we first analyzed the CHC profiles during sexual maturation. The oocytes of female cockroaches mature after eclosion by taking up vitellogenin until ovulation [45], and females become sexually receptive and mate 4-5 days before ovulation [53]. In our study, female cockroaches oviposited late on day 7 or early day 8 (data not shown), therefore AD1–6 (adult days 1-6) adult cockroaches were used for CHC analysis. Different CHC components were identified as previously described [54]. We found no qualitative differences between males and females, but quantitative differences in CHCs became more apparent with adult age (S1 Table). At an early adult stage (AD1 and AD2), females and males had similar CHC profiles. However, differences were apparent at AD3 and gradually increased until AD6 (Figure 1A). Along with sexual maturation in males, the proportions of C27 CHCs and 9-; 11-; 13-; 15-MeC29 (male-enriched peak 17) obviously increased, while other C29 CHCs, particularly 3,7-; 3,9-; 3,11-DimeC29 (female-enriched peak 24) significantly decreased. In females, however, the CHC profiles consistently displayed high proportions of C29 CHCs and especially 3,7-; 3,9-; 3,11-DimeC29 (Fig 1B–E). Principal component analysis (PCA) showed that the male and female CHC profiles were more similar at AD1, but diverged at AD6, and the divergence was mainly reflected in principal component 2 which largely represents the chain length factor (Fig 1F–G). The sexual dimorphism of CHCs was generated at the adult stage (nymphal CHC chromatogram showed no qualitative differences between males and females, S1 Fig), and the sexes diverged with sexual maturation. Notably, the differences between male and female CHC profiles suggested that chain length is an important factor in sexual dimorphism of CHCs.

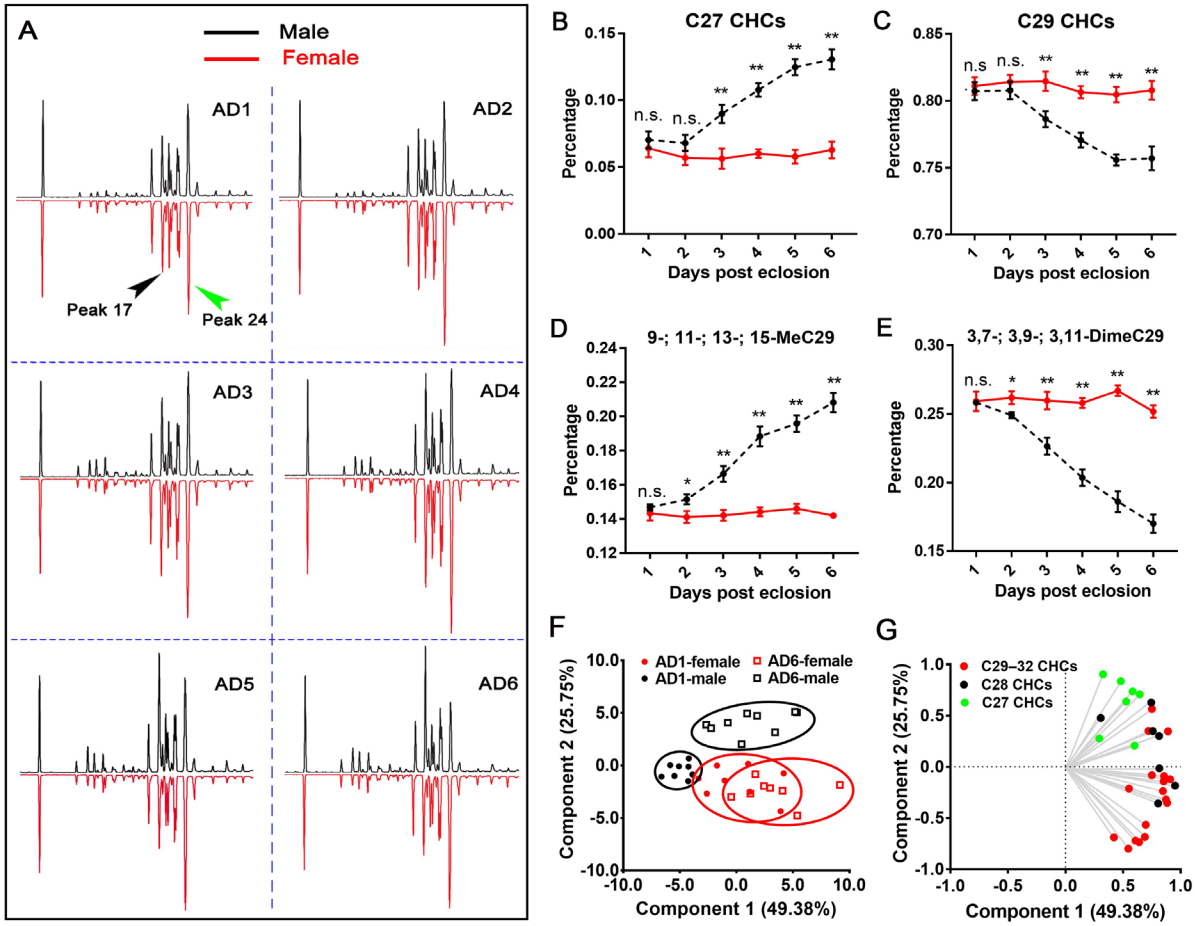

Fig 1. Development of sexually dimorphic cuticular hydrocarbons. **(A)** Comparisons of 1- to 6-day-old adult (AD1–AD6) male (black) and female (red) cuticular hydrocarbon profiles. The first peak represents the internal standard *n*-hexacosane. Other peaks correspond to the CHCs in S1 Table. Peak 17 is male-enriched (9-; 11-; 13-; 15-MeC29) and gradually increased with age in males. Peak 24 is female-enriched (3,7-; 3,9-; 3,11-DimeC29). The proportions of C27 CHCs **(B)**, C29 CHCs **(C)**, Peak 17 **(D)**, and Peak 24 **(E)** in the total CHCs from AD1 to AD6 were compared between males (black dashed lines) and females (solid red lines). Data are shown as mean ± SEM (n.s. represents no significant difference; $*P < 0.05$, $**P < 0.01$, two-tailed Student's *t*-test, n = 8–10). **(F, G)** Principal component analysis of AD1 and AD6 CHC profiles of males and females. In **(F)**, each dot represents a datum calculated from one cockroach. AD1 male (black solid circles) and female (red solid circles) CHC profiles overlapped, whereas AD6 male (black open square) and female (red open square) CHC profiles separated along PC2. In the loading diagram **(G)**, CHCs with different chain lengths are marked by green (C27), black (C28), and red (C29–C32), showing that C27 CHCs vectored toward males along PC2, whereas longer chain CHCs vectored toward females.

153 ## *BgElo12* and *BgElo24* are involved in HC biosynthesis

154 The genetic basis of HC production in *B. germanica* is not completely understood. Our previous work
155 identified a fatty acid synthase gene (*BgFas1*) and a P450 oxidative decarbonylase gene (*CYP4G19*) that are
156 involved in HC biosynthesis, but both showed no function in the sexual dimorphism of CHCs [55,56]. In this
157 study, we found that the differences of CHCs between females and males are largely reflected in carbon chain
158 length, which suggests that elongase genes may be the crucial regulator of SDCHCs. This was consistent
159 with specific C29 CHCs reported to be enriched in females, and C27 CHCs enriched in males [52]. Based on
160 this assumption, we searched for potential *BgElo* genes in the *B. germanica* genomic data and our full length
161 transcriptomic data [56,57]. A total of 24 different *BgElo* candidate genes were identified, and all *BgElos*
162 were cloned and re-sequenced. Sequence alignment revealed that different BgElo proteins showed high
163 homology and contained the conserved HXXHH and YXYY motifs [58]. All BgElo proteins displayed an
164 ELO domain and several transmembrane domains (S1 Appendix).

165 The fatty acid precursors used for HC production generally originate in the oenocytes, but also can be
166 transported from the fat body to oenocytes [29]. Therefore, we first analyzed the transcript levels of all *BgElos*
167 in the fat body and abdominal integument. Results showed that *BgElo24* and *BgElo12* were highly expressed
168 in the integument, and *BgElo1*, *2*, *3*, *6*, *7*, *9*, *10*, *11*, *14*, *17*, *20*, and *22* were also abundant in the integument,
169 while other *BgElos* were nearly undetectable (Fig 2A). In the fat body, *BgElo10* and *BgElo22* were highly
170 expressed, *BgElo1*, *2*, *3*, *11*, *12*, and *24* were slightly expressed, and other *BgElos* were undetectable (Fig
171 2B).

172 Based on these results, RNAi of the genes that were expressed in the abdominal integument or fat body
173 was performed. A first injection of dsRNA was performed in early fifth-instar nymphs (N5D1 or N5D2), and
174 a boost injection was performed one week later, and then the treated cockroaches were collected at different
175 adult stages and subjected to CHC analysis. RNAi of different *BgElo* genes significantly decreased the
176 mRNA level (S2 Fig). GC–MS analysis of CHCs showed that C27 CHCs were affected by many genes –
177 knockdown of *BgElo1*, *10*, *12*, *14*, *20*, and *24* caused a significant increase in C27 CHCs, and repression of
178 *BgElo12* showed the greatest increase of the content of C27 CHCs (Fig 2C). C28 CHCs were rarely affected,
179 with only knockdown of *BgElo24* causing a significant decrease in C28 CHCs (Fig 2D). C29 CHCs were the
180 most abundant in *B. germanica*, and only RNAi of *BgElo12* or *BgElo24* significantly decreased their amount
181 (Fig 2E). RNAi of *BgElo12* or *BgElo24* also dramatically decreased the amount of C30 CHCs, while RNAi

of *BgElo2* increased C30 CHCs (Fig 2F). CHCs with chain lengths greater than 30 occur in low quantities in *B. germanica*, but the most striking result was a sharp decline that resulted from *BgElo24*-RNAi (S3 Fig). The detailed changes of individual CHCs after RNAi of *BgElos* are available in S2 Table. In conclusion, these data strongly suggest that *BgElo12* and *BgElo24* are involved in CHC production, but we cannot rule out that other *BgElo* genes might have a less prominent role in HC biosynthesis.

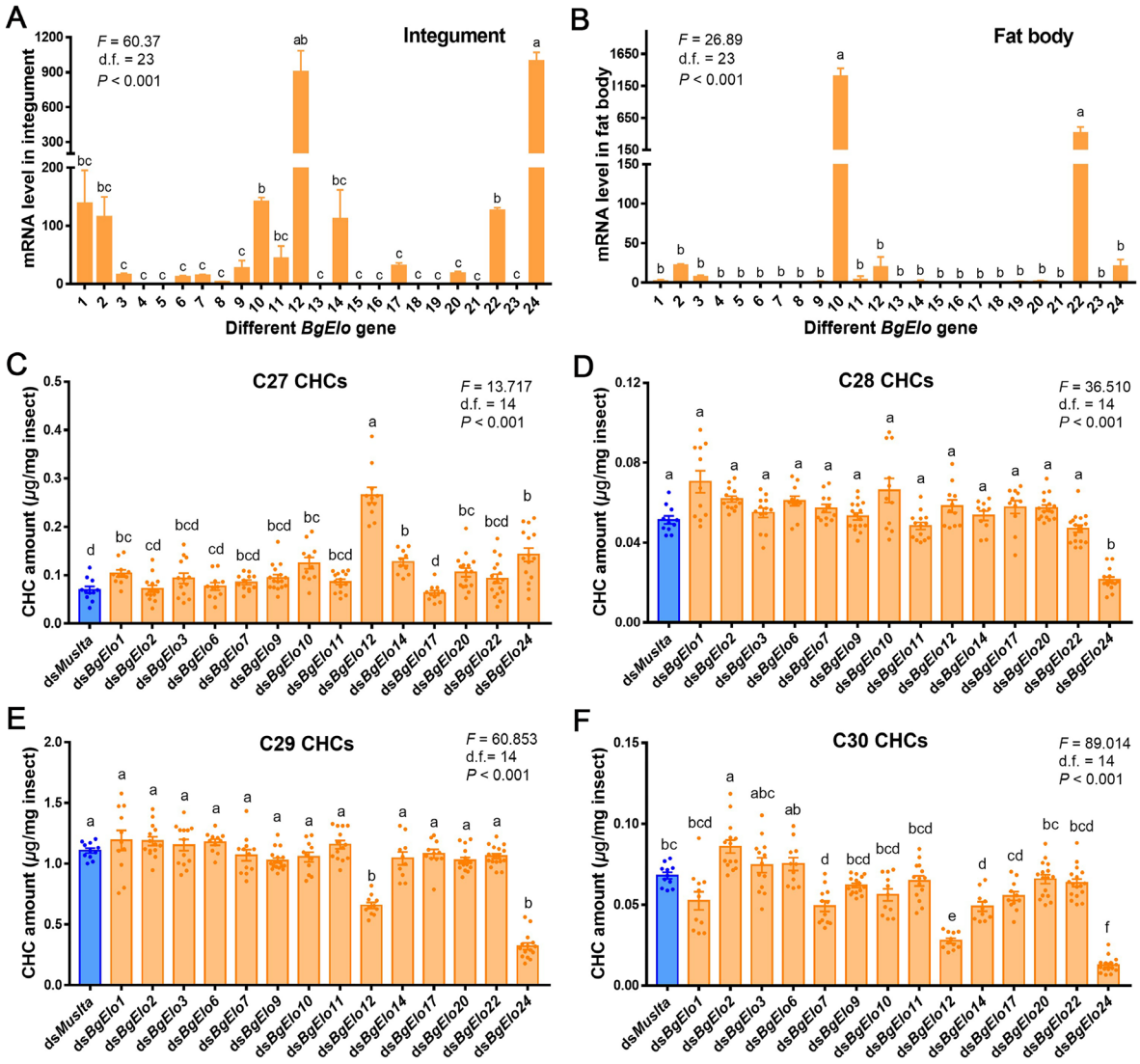

Fig 2. RNAi screen to identify *BgElo* genes involved in long-chain cuticular hydrocarbon biosynthesis. Transcript levels of different *BgElo* genes in the abdominal integument **(A)** and fat body **(B)**. The numbers on the abscissa correspond to *BgElo1–24*. Data are shown as mean ± SEM, and calculated from 4 replicates (each replicate contains 4 cockroaches for the integument and 8 cockroaches for the fat body). The influence of knockdown of different *BgElo* genes on C27 **(C)**, C28 **(D)**, C29 **(E)**, and C30 **(F)** CHCs is shown. Data are presented as mean ± SEM and calculated from 10–16 AD2 female cockroaches, each dot indicating a single datum from one cockroach.

194 Only RNAi of *BgElo12* and *BgElo24* resulted in significant increases of C27 CHCs and decreases of C29 CHCs.
195 Different letters indicate statistically significant differences between groups using Welch's ANOVA (Games-
196 Howell multiple comparisons test, $P < 0.05$).
197

198 ## *BgElo12* is the terminal gene in maintaining sexually dimorphic hydrocarbon profiles

199 Although, it appears that both *BgElo12* and *BgElo24* are involved in HC production, it is unclear which
200 gene is responsible for sexual dimorphism of CHCs. Therefore, we compared the CHC profiles of treated
201 female cockroaches with wild type male cockroaches. The results showed that only RNAi of *BgElo12* made
202 the female CHC profile more similar to the male profile (Fig 3A), reflected by a significant increase of C27
203 CHCs without affecting the male-enriched peak 17, and a selective downregulation of C29 CHCs, with a
204 dramatic downregulation of the female-enriched peak 24 and some other C29 CHCs (Fig 3B). Also,
205 knockdown of *BgElo12* increased the proportions of C27 CHCs and peak 17, while the proportions of C29
206 CHCs and peak 24 significantly decreased (Fig 3D). These changes converged the female CHC profile
207 toward the male CHC profile. The repression of *BgElo24* downregulated all C28–C32 CHCs (Fig 3C), even
208 though knockdown of *BgElo24* increased the proportion of C27 CHCs, and decreased the proportion of C29
209 CHCs and peak 24 (Fig 3E); the amount of the male-enriched peak 17 was also dramatically downregulated
210 (Fig 3C). Similar results were generated in males, and RNAi of *BgElo12* generated the characteristics of male
211 CHC profiles (S4A Fig), while *BgElo24*-RNAi downregulated all C28–C32 CHCs (S4B Fig). In order to
212 confirm these results, a second RNAi target was used for both genes, and similar results were generated (S5A
213 and S5B Fig). In addition, we analyzed the internal HCs after repression of *BgElo12* or *BgElo24*. The internal
214 HCs underwent similar changes as CHCs (S5C and S5D Fig). These results suggest that the changes imposed
215 by *BgElo12*- or *BgElo24*-RNAi were caused by a deficiency in *de novo* HC biosynthesis and not the transport
216 of HCs from internal tissues to the cuticle.

217 We also examined the spatio-temporal expression of *BgElo12* and *BgElo24*. Both *BgElo12* and *BgElo*
218 *24* were primarily expressed in the abdominal integument, where the oenocytes that produce HCs are located
219 (S6 Fig). Monitoring of *BgElo12* expression in females and males across different developmental stages
220 showed that female and male *BgElo12* mRNA levels were similar at N6D4 and early adult stage, but its
221 expression level was higher in females than in males at AD3, and the difference increased through AD6 (Fig
222 3F), a pattern similar to the production of SDCHCs. The expression levels of *BgElo24* were higher in males

than in females starting at AD2 (Fig 3G). These results also support that only *BgElo12*, and not *BgElo24*, is involved in sexual dimorphism of CHCs in *B. germanica*.

Finally, because CHCs are important waterproofing agents in insects [18], we investigated the roles of *BgElo12* and *BgElo24* in desiccation resistance. We found that repression of *BgElo24* dramatically decreased tolerance of desiccation, but RNAi of *BgElo12* had little effect on desiccation tolerance (Fig 3H). These results indicate that the biological significance of *BgElo12* in cockroaches is to support sexual dimorphism of CHCs, whereas *BgElo24* supports desiccation tolerance.

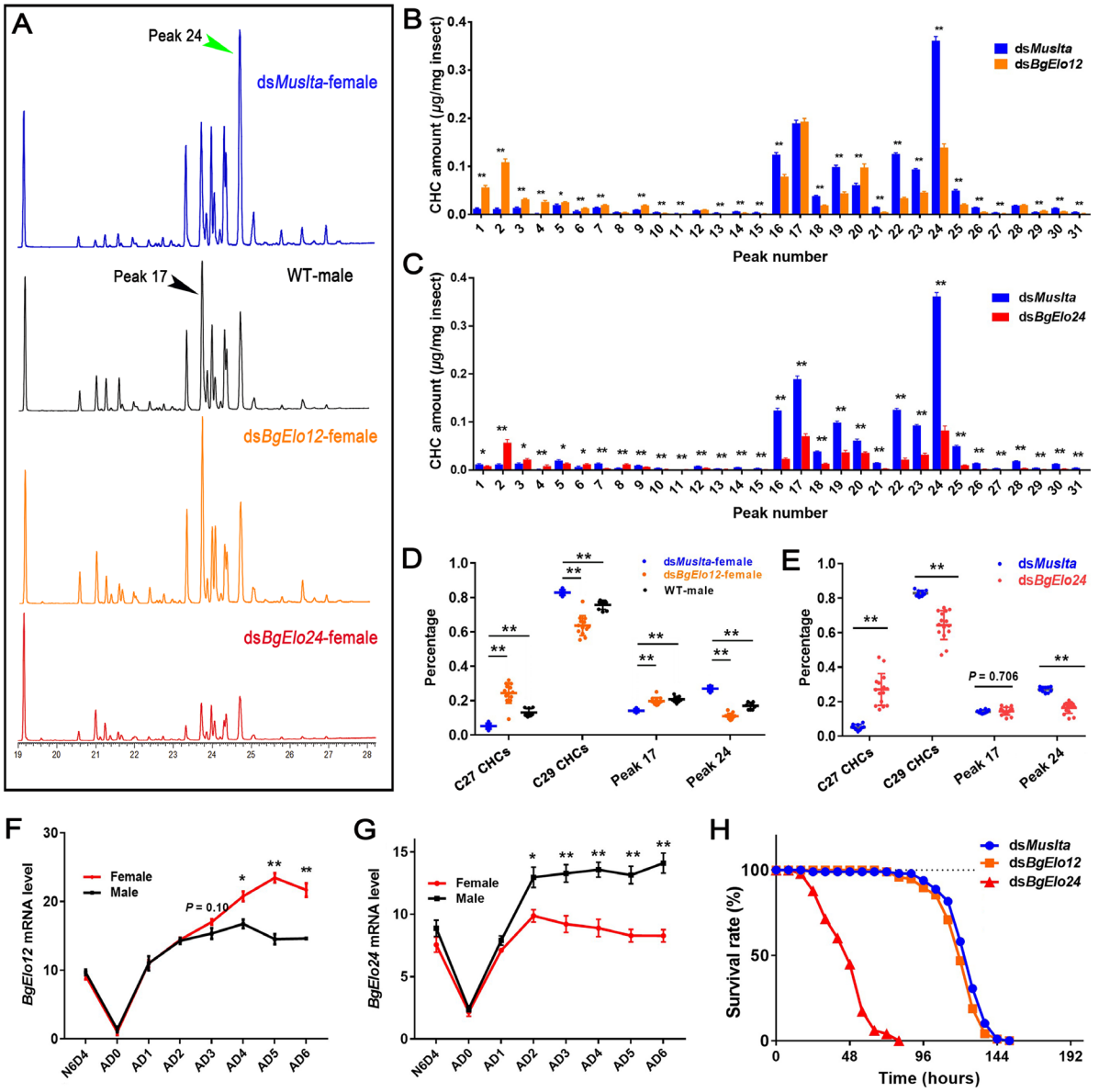

Fig 3. *BgElo12* is involved in generating sexually dimorphic hydrocarbons. **(A)** Gas chromatogram of CHC profiles from differently treated cockroaches. The CHC profiles of sexually mature females and males (AD6–AD8) showed a marked difference, and RNAi of only *BgElo12* in females generated a male-like CHC profile.

234 Quantitative influence of *BgElo12*-RNAi **(B)** and *BgElo24*-RNAi **(C)** in females on the amount of each CHC.
235 Percentage change of the C27 CHCs, C29 CHCs, male-enriched peak 17, and female-enriched peak 24 after
236 *BgElo12*-RNAi **(D)** or *BgElo24*-RNAi **(E)**. Data in **(B–E)** are shown as mean ± SEM, $*P < 0.05$, $**P < 0.01$; two-
237 tailed Student's *t*-test, n = 10 for *dsMuslta*, 11 for *dsBgElo12*, and 15 for *dsBgElo24*, 9 for wild type males (WT-
238 male). Relative expression of *BgElo12* **(F)** and *BgElo24* **(G)** among different developmental stages and different
239 ages of adult males and females. *P* values were calculated from 4 replicates (2–3 cockroaches/replicate), $**P <$
240 0.01; two-tailed Student's *t*-test. **(H)** Survival rates of *dsMuslta* (n = 98), *dsBgElo12* (n = 96), and *dsBgElo24* (n
241 = 98) treated female cockroaches maintained at 5% RH. Survival rates were calculated every 8 h until all
242 cockroaches died.
243

244 BgElo24 provides VLCFA substrates for BgElo12

245 Thus far, we showed that both *BgElo12* and *BgElo24* are involved in HC production, RNAi of *BgElo12*
246 only selectively decreased some HCs while repression of *BgElo24* dramatically downregulated all C28–C29
247 HCs, and some HCs were affected by both *BgElo12* and *BgElo24*. We also found that knockdown of *BgElo24*
248 caused a two-fold upregulation of *BgElo12*, while RNAi of *BgElo12* had no significant influence on *BgElo24*
249 mRNA level (S7A and S7B Fig). Therefore, we considered whether BgElo24 is a basic elongase that provides
250 substrates used for HC biosynthesis, and if BgElo24 generates primary precursors that can be further
251 catalyzed by BgElo12. We verified the functions of BgElo12 and BgElo24 in VLCFA biosynthesis with
252 heterologous expression of *BgElo12* and *BgElo24* in *Saccharomyces cerevisiae* (strain INVSc1). The genetic
253 background of *S. cerevisiae* is relatively clear, as wild type *S. cerevisiae* contains three different ELO proteins:
254 ELO1 is able to elongate C14 FAs to C16 FAs, ELO2 can generate C24 FAs, and ELO3 plays essential roles
255 in the conversion of C24 FAs to C26 FAs [59,60]. In our study, activation of GAL1 promoter by galactose
256 successfully transcribed the target genes, and we detected the expression GFP protein (S7C–E Fig). GC–MS
257 analysis of FAs in *S. cerevisiae* that contained pYES2-GFP (control) detected large amounts of C16:1, C16:0,
258 C18:1, and C18:0 FAs, minor amounts of C20–C24 and C28 FAs, and a larger amount of C26:0 FAs (S3
259 Table). Yeast with exogenous *BgElo12* did not produce any new FAs, but heterologous expression of
260 *BgElo24* sharply increased the amount of C28:0 FA, and generated a new component, C30:0 FA (Fig 4A–C;
261 S7H and S7I Fig). These results suggest that BgElo24 is capable of elongating endogenous yeast FAs to
262 generate C28:0 and C30:0 FAs.

263 Considering that BgElo12 and BgElo24 may selectively elongate substrates with specific carbon chain
264 lengths, we separately added C20:0, C22:0, C24:0, C26:0, and C28:0 FAs to the medium. Compared with
265 the control, BgElo24 did not produce any new FAs when C20:0, C22:0, C24:0, or C26:0 were added (S3
266 Table). However, when C28:0 FA was added, yeast with pYES2-BgElo12 generated C30:0 FA, although in
267 small amounts (Fig 4A'–C', S3 Table). These results suggest that BgElo24 not only directly provides
268 substrates (C28 and C30 fatty acyl-CoAs) for the biosynthesis of C27 and C29 *n*-alkanes, but also provides
269 C28 fatty acyl-CoA for BgElo12 to elongate to C30 fatty acyl-CoA, which in turn generates C29 *n*-alkane.
270 This might be the reason why *in vivo* RNAi of *BgElo12* slightly decreased C29 *n*-alkane and caused a
271 dramatic increase in C27 *n*-alkane, whereas RNAi of *BgElo24* dramatically decreased C29 *n*-alkane.
272 In order to analyze the activity of BgElo12 and BgElo24 in elongating methyl-branched FAs, two
273 representative substrates, 2-MeC16:0 and 14-MeC16:0 FAs, the potential substrates for 15-methyl HCs and
274 3-methyl HCs, respectively, were added to the medium. However, we found that these substrates could not
275 be catalyzed by BgElo12 or BgElo24 (S7F–F'' Fig and S7G–G'' Fig). We suspect that this might be caused
276 by a shortcoming of the yeast FA elongation system. FA elongation requires an elongase and three other
277 enzymes including a 3-keto-acyl-CoA-reductase, a 3-hydroxy-acyl-CoA dehydratase, and a trans-enoyl-
278 CoA-reductase [29]. The last three yeast-endogenous enzymes may not catalyze methyl branched substrates.
279 In conclusion, these results indicate that both BgElo12 and BgElo24 catalyzed the biosynthesis of VLCFAs
280 in the yeast heterologous system, and BgElo24 was able to provide primary substrates for BgElo12. However,
281 the activity of BgElo12 and BgElo24 in methyl-branched FA elongation needs further investigation.
282

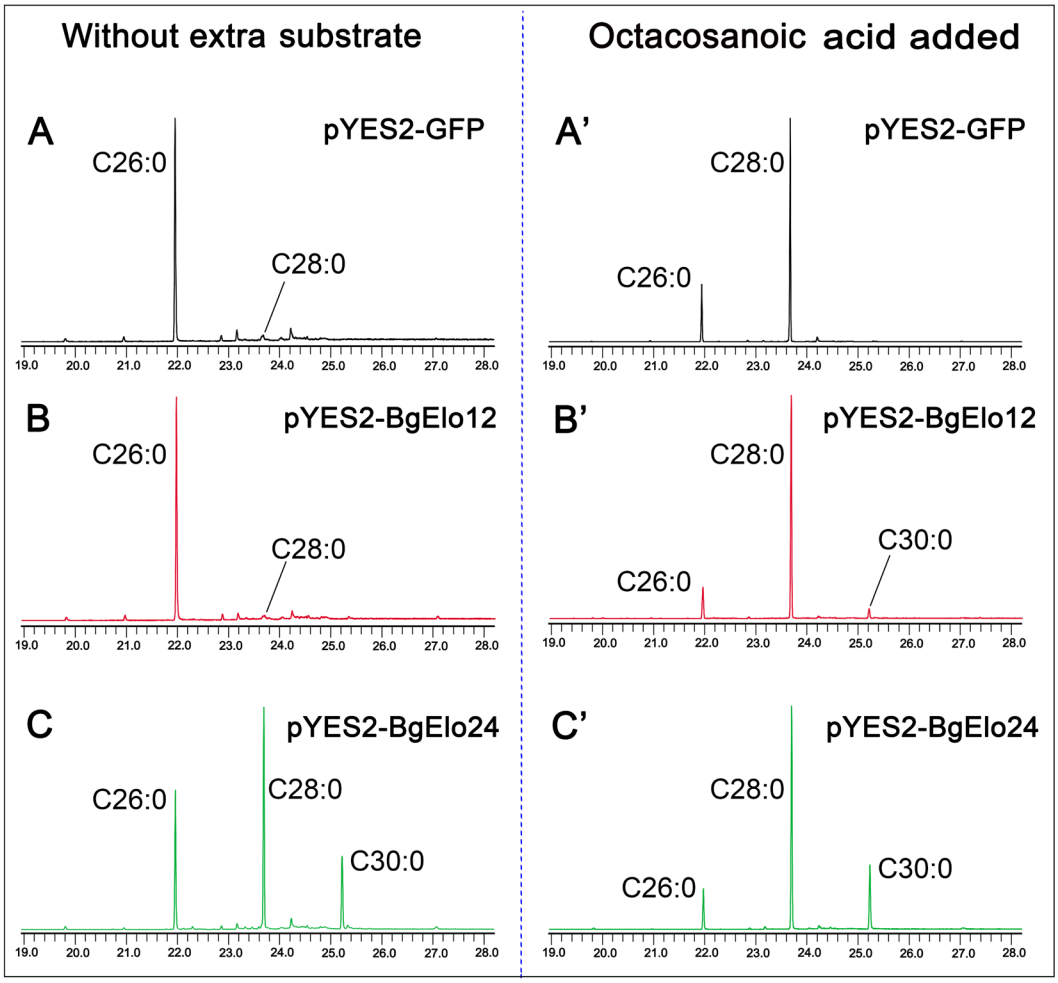

Fig 4. Yeast expression and substrate catalysis of BgElo12 and BgElo24. Representative gas chromatogram of fatty acid methyl esters of yeast transformed with pYES2-GFP **(A)**, pYES2-BgElo12 **(B)**, and pYES2-BgElo24 **(C)** without addition of extra substrates. After adding octacosanoic acid (C28:0), the corresponding chromatograms are shown at the right for pYES2-GFP **(A')**, pYES2-BgElo12 **(B')**, and pYES2-BgElo24 **(C')**. The chromatograms are truncated, and only chromatographic peaks of interest are indicated. The FAMEs are labeled by their corresponding saturated FAs. Complete chromatograms are shown in S7 Fig.

Female-enriched HCs are crucial for contact sex pheromone-based courtship performance

The largest single chromatographic HC peak in females contains 3,7-; 3,9-; 3,11-DimeC29, which is much less represented in males. Because 3,11-DimeC29 has been shown to be the precursor for the contact sex pheromone 3,11-DimeC29-2-one (C29 methyl ketone) in *B. germanica* [48], we suspected that the

296 female-specific HC profile may be important for maintaining a high level of contact sex pheromone. We first
297 monitored the pattern of 3,11-DimeC29-2-one accumulation in the first gonotrophic cycle. The contact sex
298 pheromone showed a stable low level at the early adult stage (AD0–AD2), its accumulation started at AD3,
299 quickly increased from AD5 to AD7 (Fig 5A), but decreased at AD8 when most females oviposited (data not
300 shown). Analysis of the influence of *BgElo12*-RNAi on C29 methyl ketone was performed at AD6. Female
301 cockroaches were subjected to three consecutive dsRNA injections before being subjected to lipid analysis:
302 the first one at early fifth instar, the second at early sixth instar, and the third at AD1. We found that repression
303 of *BgElo12* reduced the C29 methyl ketone by more than 75% in both cuticular and internal extractions (Fig
304 5B–D).

305 We next determined whether the *BgElo12*-RNAi repression of pheromone production in females
306 affected male courtship behavior. When the female contact sex pheromone is detected by a male, it displays
307 a characteristic male courtship behavior, including wing-raising (WR) [50]. Importantly, this behavior can
308 be elicited by an isolated female antenna, and details of this assay, including latency and rate of WR, have
309 been described [61]. When an antenna of AD5 female was used as stimulus, nearly all males responded.
310 RNAi of *BgElo12* resulted in only a slight decline in WR rate (about 20%), but the latency of WR was
311 significantly increased (Fig 5E and 5E'). AD5 females accumulated a large amount of contact sex pheromone,
312 whereas males can be fully activated by about 10 ng of 3,11-DimeC29-2-one applied onto an antenna [62].
313 This is likely the reason why RNAi of *BgElo12* had only a small influence on WR rate. Therefore, we
314 repeated this experiment using AD3 females, which have less contact sex pheromone on the cuticle. We
315 found that males responded to 80% of the control antennae with the WR display, but less than 40% of the
316 antennae from *BgElo12*-RNAi females elicited WR in males. The average latency of WR toward antennae
317 of *BgElo12*-RNAi females was 18.03 s, while the control antennae elicited WR in 11.05 s (Fig 5F and 5F').
318 These results indicate that female-enriched HCs are advantageous for contact sex pheromone biosynthesis,
319 especially at the early sexual maturation stage.
320

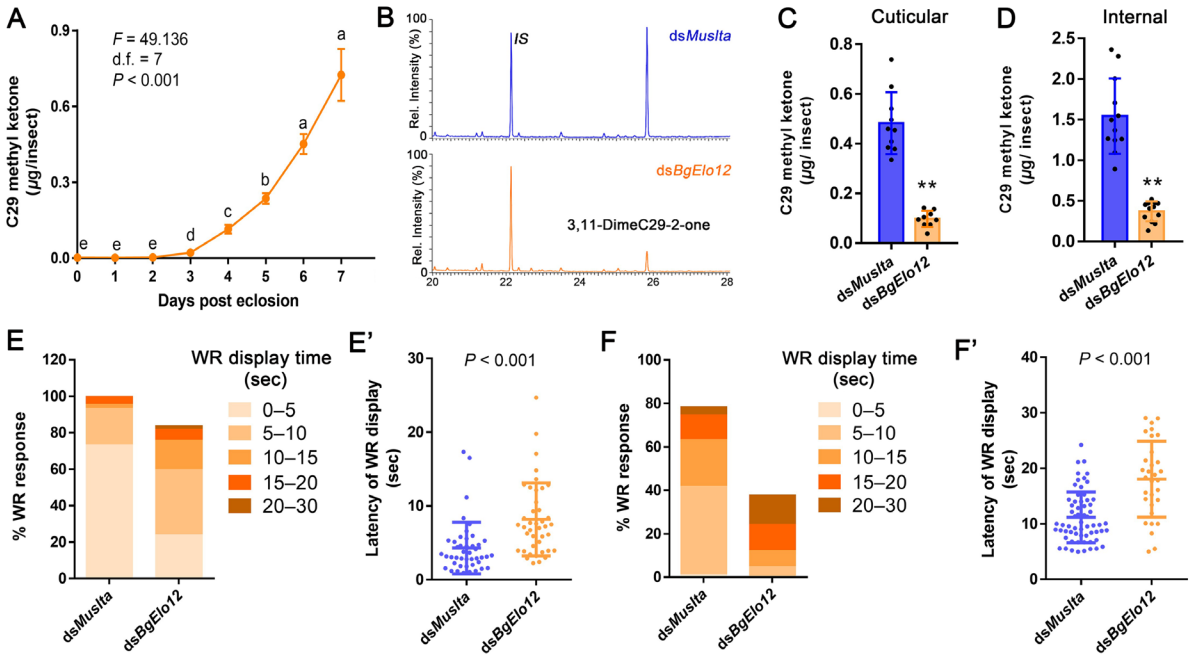

Fig 5. *BgElo12*-RNAi effects on contact sex pheromone biosynthesis in females and male courtship performance. **(A)** The pattern of contact sex pheromone (3,11-DimeC29-2-one) accumulation during female sexual maturation. Data are shown as mean ± SEM. Different letters indicate significant differences between groups using Welch's ANOVA (Games-Howell multiple comparisons test, $P < 0.05$). **(B)** Representative chromatogram showing lower amounts of sex pheromone after *BgElo12*-RNAi. *IS* is the internal standard 14-heptacosanone. Cuticular **(C)** and internal **(D)** amounts of 3,11-DimeC29-2-one (C29 methyl ketone) after *BgElo12*-RNAi. Data are shown as mean ± SD, and each replicate is shown as a dot. $^{**}P < 0.01$, two-tailed Student's *t*-test; n = 9–12. Influence of *BgElo12*-RNAi on the ability of AD5 **(E–E')** and AD3 **(F–F')** female antennae to elicit courtship in males. The percentage of males that responded with a wing-raising (WR) behavior in response to contact with female antenna were determined for 44 (*dsMuslta*) and 49 (ds*BgElo12*) female antennae in **(E)**, and 79 (ds*Muslta*) and 82 (ds*BgElo12*) antennae in **(F)**. Each female antenna was tested only once with a single male. The proportion of WR display over different time periods (latency, sec) is shown in progressively darker colors. **(E')** and **(F')** Average latency of WR display calculated from those antennae that successfully activated a courtship behavior of males within 30 s. Data are shown as mean ± SD, each dot represents a datum calculated from one antenna. *P* values were determined by two-tailed Student's *t*-test.

Sex-differentiation genes modulate *BgElo12*

The female-enriched HC composition is tightly associated with a higher expression of *BgElo12* in

340 females, but the regulators that govern sexually dimorphic expression of *BgElo12* in females and males are
341 unknown. Wexler et al. reported that RNAi of the sex-determination gene *BgTra* in females converts its CHC
342 profile to a male-like profile [52]. Taken together with our results, it would appear that the sex-differentiation
343 pathway might be involved in regulating *BgElo12* expression. We first confirmed the function of *BgTra* and
344 *BgDsx* in sex-specific development *via* RNAi. For each gene, we used two unique RNAi targets within a
345 conserved sequence region for multiple isoforms. RNAi of *BgTra* and *BgDsx* in females or males showed
346 similar phenotypes as described by Wexler et al. [52]. *BgTra* is only functional in females, while *BgDsx* only
347 works in males (S8 Fig). We next studied the expression of *BgTra* and *BgDsx* in females and males using
348 qPCR primers that target all isoforms of each gene. The expression of both *BgTra* and *BgDsx* increased after
349 eclosion, but *BgTra* transcript levels tended to be stable from AD4 to AD6 (Fig 6A and 6B). RNAi of *BgTra*
350 in females significantly decreased the mRNA level of *BgElo12*, but *BgElo12* expression was unaffected in
351 males (Fig 6C). Notably, the downregulation of *BgElo12* by ds*BgTra*-injection in females could be rescued
352 by co-injection of ds*BgTra* and ds*BgDsx* (Fig 6C), but ds*BgDsx* alone was not functional in regulating
353 *BgElo12* expression in females (Fig 6D). Conversely, in males, knockdown of *BgDsx* alone increased the
354 expression of *BgElo12* (Fig 6D). As RNAi of *BgTra* in females generated the male type *BgDsx* ($BgDsx^M$)
355 [52], we suspect that the downregulation of *BgElo12* in females after RNAi of *BgTra* was caused by the
356 generation of $BgDsx^M$. This hypothesis was supported by co-injection of ds*BgTra* and ds*BgDsx*, and a dual-
357 luciferase reporter assay that $BgDsx^M$ could directly modulate the expression of *BgElo12* by interaction with
358 its upstream sequence region (S9 Fig). Further, we found that RNAi of neither *BgTra* in females nor *BgDsx*
359 in males could affect the expression of *BgElo24* (S10 Fig), suggesting that *BgElo24* is not regulated by these
360 two sex-differentiation genes.

361 We further analyzed the effects of *BgTra* and *BgDsx* on HC profiles. Knockdown of *BgTra* in females
362 masculinized the CHC profile and increased the male-enriched CHC components; however, this change
363 disappeared by co-injection of ds*BgTra* and ds*BgDsx* (Fig 6E, 6F, and S11A Fig). Similarly, repression of
364 *BgDsx* in males feminized the CHC profile, and increased the female-enriched components (Fig6E, 6G, and
365 S11B Fig). In order to verify that the sex-differentiation genes affected CHC profiles by regulating the
366 generation of HCs but not their selective transport and deposition to the cuticle, we analyzed the internal HCs.
367 RNAi of both *BgTra* in females and *BgDsx* in males caused an inter-sexual conversion of internal HC profiles,
368 as seen in the CHCs (S12A–D Fig). Although we found little qualitative differences in the HC profiles

369 between internal and cuticular HCs, we found significant quantitative changes. For example, after RNAi
370 inhibition of *BgTra* in females, the increase of 9-; 11-; 13-; 15-MeC29 (peak 17) on the epicuticle was greater
371 than in internal tissues, while the decrease of 3,7-; 3,9-; 3,11-DimeC29 (peak 24) on the surface was less than
372 in internal tissues (S11A Fig and S12A Fig), suggesting the possibility of excessive transport of internal HCs
373 toward the cuticle after repression of *BgTra* in females. As for RNAi of *BgDsx*, an opposite change was
374 generated in males– there appeared to be less transport of HCs to the cuticle (S11B Fig and S12B Fig). Also,
375 the total amount of internal HCs was significantly decreased in *BgTra*-RNAi females, while it was increased
376 in *BgDsx*-RNAi males (S12E and S12F Fig). These results suggest that there is an unusual transport of HCs
377 after repression of *BgTar* or *BgDsx*. We suspect that the unusual transport of HCs may be caused by changes
378 in the capacity to store internal HCs, as large amounts of internal HCs are shunted to the ovaries [45,63], and
379 sex-differentiation genes are the key regulators of normal ovary development in females and repression of
380 ovary generation in males [8,52]. We conclude that although the transport of HCs from internal tissues to the
381 cuticle was affected after repressing *BgDsx* or *BgTra*, the effect was on overall HC transport, with no apparent
382 selective transport on specific HCs.

383 Overall, our results indicate that the sexual dimorphism of HCs in *B. germanica* is primarily determined
384 by *BgElo12*, and sex-determination pathway genes are the critical regulators that control the asymmetric
385 expression of *BgElo12* between males and females.

386

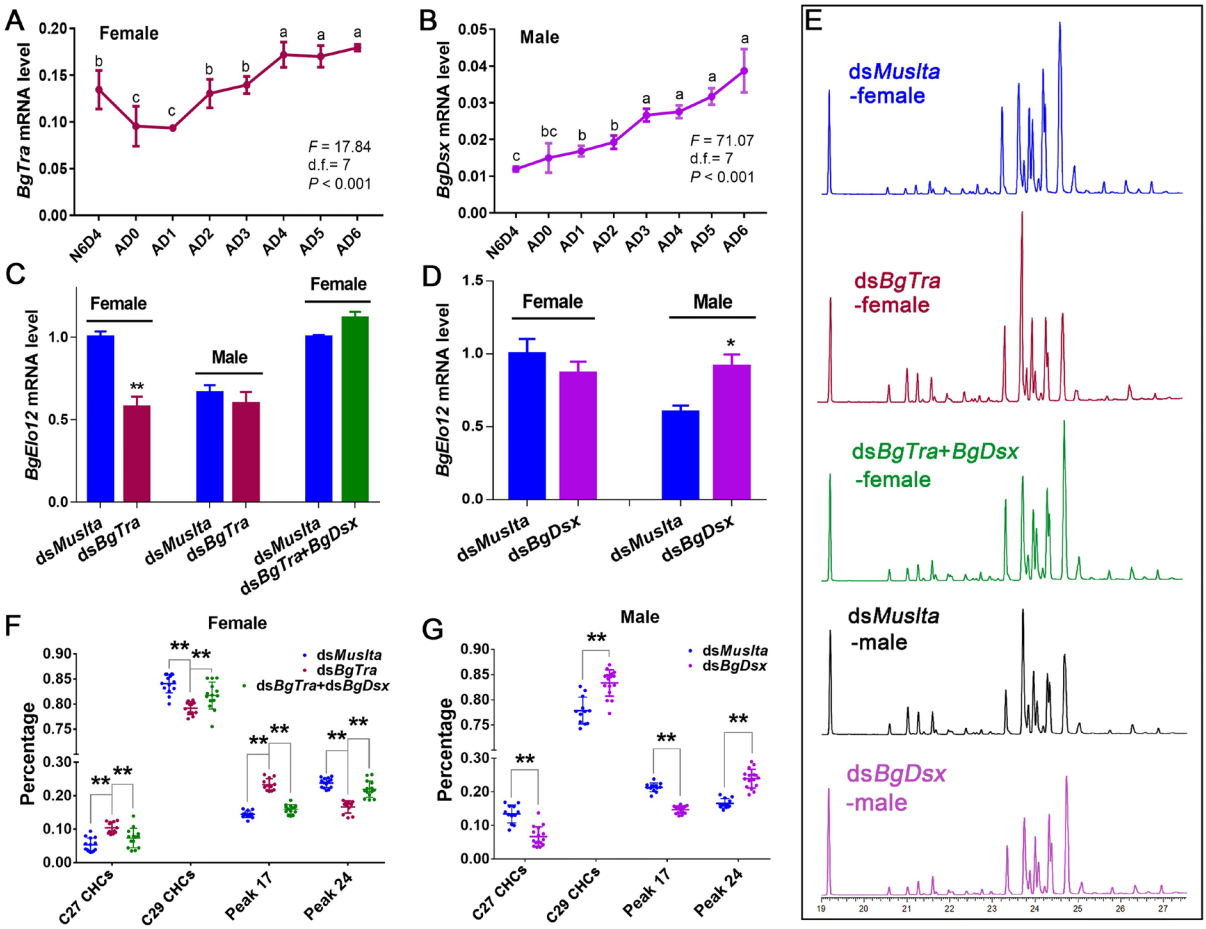

Fig 6. Regulation of *BgElo12* and sexually dimorphic hydrocarbon profiles by sex-differentiation genes. Temporal patterns of *BgTra* expression in females **(A)** and *BgDsx* expression in males **(B)**. Data are shown as mean ± SEM and calculated from 4 replicates (2–3 cockroaches/replicate). N6D4 is 6th instar nymph on day 4, AD0–6 represent adult days 0 to 6. Different letters indicate significant differences between the groups (ANOVA, Fisher's LSD, $P < 0.05$). **(C)** and **(D)** Regulation of *BgElo12* expression by *BgTra* and *BgDsx*. Data are shown as mean calculated from 4 replicates (2–3 cockroaches/replicate) ± SEM; *$P < 0.05$, **$P < 0.01$, two-tailed Student's *t*-test. **(E)** Gas chromatograms of CHCs after repressing different sex-differentiation genes. **(F)** Regulation of the proportions of representative CHCs by *BgTra* in females. Data are presented as mean ± SD, **$P < 0.01$; two-tailed Student's *t*-test; n = 14 for *dsMuslta*, 12 for ds*BgTra*, and 14 for ds*BgTra*+ds*BgDsx*. **(G)** The proportion change of representative CHCs after *BgDsx*-RNAi in males. Data are shown as mean ± SD; **$P < 0.01$; two-tailed Student's *t*-test, n = 12 for *dsMuslta* and 16 for ds*BgDsx*.

Discussion

Our study reveals a novel molecular mechanism responsible for the formation of SDHCs in *B. germanica*. The CHC profiles in insects are regulated by complex biosynthetic and transport pathways, involving multiple gene families. We demonstrated that the fatty acid elongation step is responsible for sexual dimorphism of CHCs in *B. germanica*, We identified that both *BgElo12* and *BgElo24* were participated in HC biosynthesis, but only the female-enriched *BgElo12* is the core gene that encodes for the elongase involved in generating more female-enriched HCs, and the asymmetric expression of *BgElo12* between the sexes is modulated by sex-differentiation genes: $BgDsx^{M}$ represses the expression of *BgElo12* in males, while *BgTra* removes this repression in females (Fig 7). Because a female-enriched HC serves as a precursor to a female contact sex pheromone, we also revealed the prominence of *BgElo12* in sexual behavior.

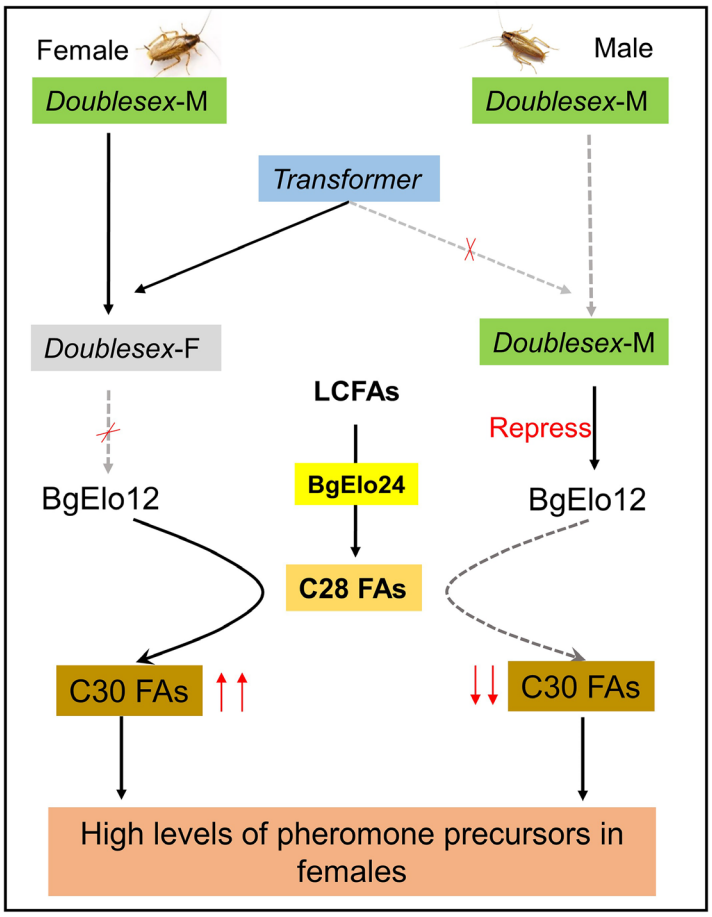

Fig 7. Model for *BgElo12* in generation sexually dimorphic hydrocarbons in *B. germanica*. Both *BgElo12* and *BgElo24* were participated in HC biosynthesis, but *BgElo24* is a basic fatty acid elongase which is able to catalyze a wide range of substrates and provides C28 FAs for *BgElo12* to generate specific C30 FAs. The male-specific *Doublesex* (*Doublesex-M*) is able to repress the transcription of *BgElo12* in males. However, *Transformer* only

415 functions in females, and can splice *Doublesex-M* to the non-functional female type *Doublesex* (*Doublesex-F*),
416 thus *BgElo12* is highly expressed in females and generates more C30 FAs. A high level of C30 FAs lastly produces
417 more contact sex pheromone precursors in females.
418

419 **Fatty acid chain elongation is a key step in the regulation of sexually dimorphic HCs in *B.***
420 ***germanica***

421 The diversity of HCs in insects is reflected in the HC carbon chain lengths, their degree of saturation,
422 and the number and positions of methyl groups [39]. HCs in *B. germanica* are composed of only alkanes and
423 methyl-branched alkanes, and the fatty acid biosynthesis gene that governs the incorporation of methyl
424 groups in the aliphatic chain showed no role in generating the sexual dimorphism of HCs in *B. germanica*
425 [55]. In this study, we found that sexually mature female cockroaches contain relatively higher amounts of
426 C29 HCs than males, whereas male cockroaches had more C27 HCs, suggesting that chain length is an
427 important factor in the dimorphism of HCs.

428 Studies of the genetic bases of HC biosynthesis in insects have demonstrated that chain lengths are
429 determined by the fatty acid elongation process: the rate-limiting enzyme elongase determines the chain
430 lengths of VLCFA products, and produces the final HCs with different chain lengths [30]. In our study, an
431 RNAi screen identified that *BgElo12* and *BgElo24* were involved in HC biosynthesis. Expression of both
432 genes in yeast demonstrated that both BgElo12 and BgElo24 displayed functions similar to ELOVL4 in
433 mammals, which showed a special function in the biosynthesis of VLCFAs with chain lengths greater than
434 C28 [64]. *BgElo24*, however, is a more fundamental elongase that seems able to catalyze a wide range of
435 substrates to generate FAs of various chain lengths, and can also provide primary substrates for BgElo12 to
436 produce C30 FAs. Notably, only *BgElo12* had higher expression in females, which was consistent with the
437 higher amounts of C29 HCs in females. Knockdown of *BgElo12* in females caused a dramatic decrease of
438 the female-enriched peak 24 (3,7-; 3,9-; 3,11-DimeC29) but it did not affect the male-enriched peak 17 (9-;
439 11-; 13-; 15-MeC29), which generated a male-like HC profile; however, RNAi of *BgElo24* unselectively
440 downregulated all C28–30 HCs, indicating that only *BgElo12* was involved in the formation of SDHCs in *B.*
441 *germanica*. Lastly, we found both RNAi of *BgElo12* and *BgElo24* increased some C27 HCs, indicating that
442 there are some other *BgElos* involved in HC production. The identification of these genes will be arduous,
443 because the C27 compounds occur in small amounts, and multiple BgElos may catalyze the synthesis of the

444 same HC independently. It is worth noting in this regard that *Blattella asahinai*, a sister species of *B.*
445 *germanica* produces almost no C27 compounds [65]. These two species can hybridize, potentially offering a
446 resource for the genetic regulation of C27 HCs.

447 In *B. germanica*, as in other insects, HCs are transported through the haemolymph and selectively
448 incorporated into or deposited on various tissues, including the cuticle, ovaries and specialized pheromone
449 glands [47,66,67]. In our study, analysis of the influence of *BgElo12*-RNAi on internal HCs demonstrated
450 that the female- and male-specific CHC profiles were not caused by selective transport, but rather by
451 differences in *de novo* HC biosynthesis between the sexes, regulated by *BgElo12*. Elongases have been shown
452 to participate in HC production in several other insect species including *D. melanogaster*, *Nilaparvata lugens*,
453 and *Locusta migratoria* [33,68,69]. The elongase gene *eloF* was also shown to be specifically expressed in
454 females, and might be associated with the sex-differentiation gene *Transformer*, but the reason why it cannot
455 be transcribed in male flies is not very clear [33]. Nevertheless, the roles of elongase genes in sexual
456 dimorphism of HCs in other insects have not been described.

457

458 ***BgElo12* and *BgDsx^M* are key nodes connecting the hydrocarbon synthesis and sex-**
459 **differentiation pathways**

460 In this study, we first demonstrated that *BgElo12* is the key regulator in the HC biosynthesis pathway,
461 responsible for the differences in the HC profiles between females and males. We next explored the upstream
462 regulators that modulate the sexually dimorphic expression of *BgElo12*. The molecular genetic switches that
463 determine which sex-determination pathway is followed by males and females are highly variable in animals.
464 The *doublesex/mab-3 related* (*Dmrt*) family of transcription factors includes conserved developmental
465 regulators in the sex-differentiation pathway, governing the fate of sexually dimorphic traits in animals [8].
466 *Doublesx* (*Dsx*) in arthropods, which is related to *Dmrt*, works through sex-specific splice variants that are
467 controlled by *Tra* in many insects. Sex-specific *Dsx* isoforms promote sexual differentiation by modulating
468 diverse downstream genes; thus, the *Dsx* gene is regarded as a central nexus in sexual differentiation [70,71].
469 Previous work reported that knockdown of *BgTra* converted the female cockroach CHC profiles to male-like
470 profiles [52]. In our study, RNAi of *BgTra* in female cockroaches indeed downregulated the expression of
471 *BgElo12*, but the effect of *BgTra*-RNAi on *BgElo12* expression could be recovered by co-injection of
472 ds*BgTra* and ds*BgDsx*, and RNAi of *BgDsx* in males upregulated *BgElo12* transcripts. These results suggest

473 that *BgDsx*^{M} can repress the transcription of *BgElo12* in males, and the downregulation of *BgElo12* by
474 repressing *BgTra* was caused by the conversion of *BgDsx*^{F} to *BgDsx*^{M}, as *BgTra* is able to regulate the splicing
475 of *BgDsx*^{M} to *BgDsx*^{F} [52]. The regulation of *BgElo12* by *BgDsx* connects the sex-differentiation pathway
476 with the HC biosynthesis pathway, and therefore enables the sexual dimorphism of HCs in *B. germanica*.

477 Although the dual-luciferase reporter gene assay suggested that *BgDsx*^{M} can directly regulate the
478 transcript of *BgElo12*, there may be other indirect regulatory pathways. Several candidate factors have been
479 shown to regulate the HC profiles in various insects (e.g., *D. melanogaster*), including ecdysone, juvenile
480 hormone (JH), biogenic amines, and the insulin signaling pathway [72–78]. These connections are
481 highlighted by ecdysone, which is mainly produced by the prothoracic gland, but in some insects also by the
482 ovaries [79,80], and the development of the ovaries is under the regulation of the sex-differentiation pathway.
483 Moreover, endocrine signals like JH and insulin are also regulated by the sex-differentiation pathway [81].
484 Therefore, these signals may be potential mediators that complete the regulatory network between *BgDsx*
485 and *BgElo12*. However, more detailed investigations are needed to thoroughly elucidate the differential
486 regulation of HC production in both females and males.

487 *Dsx* also regulates the HC biosynthesis pathway in *D. melanogaster*; *Dsx*^{F} specifically activates the
488 transcription of *desatF* and generates pheromonal dialkenes [42]. However, *BgDsx* operates differently in *B.*
489 *germanica* that *BgDsx*^{M} suppresses female traits in male cockroaches, and *BgTra* is important in removing
490 the inhibitory effect of *BgDsx*^{M} in females [52]. Thus, *BgDsx*^{M} represses the expression of *BgElo12*, and
491 therefore it represses the generation of female-enriched HCs in males, and *BgTra* is crucial in maintaining
492 female-enriched HCs, especially for the contact sex pheromone precursors. However, *BgTra* affects contact
493 sex pheromone biosynthesis in female cockroaches through additional pathways. We found that RNAi of
494 *BgTra* in females dramatically decreased the expression of the JH-responsive *Krüppel homolog 1*, *Krh1*, a
495 zinc-finger transcription factor (S13 Fig). JH can activate the expression of a putative sex-specific and rate-
496 limiting cytochrome p450 that catalyzes the hydroxylation of 3,11-DimeC29 to 3,11-DimeC29-alcohol,
497 which is then oxidized to the methyl ketone pheromone [48,82], and we found that JH performed this function
498 *via Krh1* (our unpublished data). Therefore, the influence of *BgTra* on contact sex pheromone biosynthesis
499 is explained not only by its effects on precursor synthesis, but also by the transition of precursors to methyl
500 ketones.

501

502 **Biological significance of the sexual dimorphism of HCs**

503 Sexually dimorphic traits are generated in females and males in response to intra- and inter-sexual
504 selection, but pleiotropic traits are also subject to natural selection, especially when they are also shaped by
505 and adapted to environmental stresses [3,83]. Most insect sex pheromones are C12-18 aldehydes, alcohols
506 and acetate esters, derived from fatty acids in specialized pheromone glands. These pheromones appear to
507 have no other function beyond attracting the opposite sex. In contrast, CHC pheromones appear to serve both
508 in sexual communication and in waterproofing of the cuticle. The female-specific contact sex pheromone of
509 *B. germanica* is clearly subject to both natural and sexual selection because it is derived from a prominent
510 CHC, which also serves as a waterproofing component of the CHC profile and is maternally invested in
511 offspring [84]. Thus, maintenance of HC contact sex pheromone precursors in female cockroaches is adaptive
512 in both reproductive success and survival in an arid environment. The quality of insect pheromones is
513 considered an honest indicator of fitness potential [75]. This assertion may be particularly pertinent in *B.*
514 *germanica*, where the pheromone and its HC precursor serve in sexual communication, resilience to
515 environmental stressors, and in maternal investment in eggs.

516 In systems that use CHCs in sexual communication, it is common for the CHC profiles to contain
517 female- and male-specific components, as is evident in *Drosophila*. In *B. germanica*, as well, male
518 cockroaches have a unique CHC profile, especially enriched in C27 components with 9-; 11-; 13-; 15-MeC29
519 being particularly prominent. The male-specific HC profile is generated during sexual maturation, suggesting
520 that it may function in sexual communication. It is possible that the male-enriched 9-; 11-; 13-; 15-MeC29
521 may function as a sex pheromone in three related contexts: a) it may distinguish males and females within
522 cockroach aggregations; b) it may signal "maleness" and male quality to females; and c) it may function in
523 male-male recognition, contests and competition for access to females. Moreover, it is possible that male-
524 specific P450s may catalyze the oxidation of these male-enriched HCs to homologous methyl ketones, as in
525 females, and in turn serve these functions. However, more bioassays are required to analyze the biological
526 significance of male-specific CHC profiles.

527 # Materials and Methods

528 ## Insect rearing

529 The German cockroach, *Blattella germanica* originated from a laboratory strain collected in the 1970s.
530 The cockroaches were maintained in aquaria at 30 ± 1ºC with a relative humidity (RH) of ~ 50% under 12:
531 12 h light–dark photoperiod regime, and fed rat chow and tap water. Newly hatched cockroaches were
532 separated and reared in new containers. Early stage (day 1 or 2) fourth- and fifth-instar nymphs were
533 separated and used in dsRNA injection; newly emerged adults were collected and reared in plastic jars for
534 experiments.

535

536 ## Preparation of HCs and methyl ketones

537 *Blattella germanica* cuticular lipids were extracted as described [64]. Individual adult female
538 cockroaches were sacrificed by freezing at −20ºC, thawed at room temperature, the cuticle surface-extracted
539 in 1 mL of hexane twice, and finally rinsed in 1 mL of hexane. *n*-Hexacosane (15 μg) or 14-heptacosanone
540 (0.5 μg) were added as internal standards. The extracts were combined and reduced to ~300 μL with a
541 nitrogen flow and loaded onto a Pasteur pipette silica gel mini-column, as previously described [55]. The
542 cuticular hydrocarbons were eluted with 8 mL of hexane, and the contact sex pheromone fraction was
543 subsequently eluted with 8 mL of 3% ethyl ether in hexane. Internal lipids were extracted from the cockroach
544 following a procedure described by Fan et al. [85]. Each surface-extracted cockroach was homogenized in a
545 solution of hexane–methanol–ddH2O (2:1:1 mL), 30 μg of *n*-hexacosane and 1 μg of 14-heptacosanone were
546 added for quantification of internal HCs and methyl ketones, respectively. The homogenate was vigorously
547 vortexed and centrifuged at 2500 g for 10 min. The supernatant hexane phase was collected and the extraction
548 was repeated using n-hexane. Separation of HCs and methyl ketones was performed using column
549 chromatography, as described above.

550

551 ## Gas chromatography–mass spectrometry (GC–MS) analysis

552 Lipid analysis was performed with a TRACE 1310 GC–ISQ single quadrupole MS (Thermo Fisher
553 Scientific, Waltham, MA, USA). In brief, lipids were separated on a DB-5MS capillary column (30 m length,
554 0.25 mm ID, 0.25 μm film thickness; Agilent Technologies, Santa Clara, CA, USA). The oven started at

555 60°C and kept for 2 min, heated to 160°C for HCs and methyl ketones, or 220°C for fatty acid methyl esters
556 (FAMEs) at a rate of 30°C/min, then increased at 3°C/min up to 250°C, followed by 10°C/min up to 320°C
557 and held for 5 min. Electron ionization mode (70 eV) was used, and the MS scan range was 45–650 m/z at a
558 rate of 5 scans/s. Identification of compounds and peak area determination was performed with a Xcalibur
559 2.2 workstation.
560

561 **RNA isolation and real time-quantitative PCR (RT-qPCR)**

562 Total RNA was isolated with RNAiso Plus Reagents (Takara, Dalian, Liaoning, China) according to the
563 manufacturer's instructions. cDNA was reverse-transcribed from 800 ng of total RNA using the
564 PrimeScript™ RT reagent Kit with gDNA Eraser (Takara). Gene-specific primers with appropriate
565 amplification efficiency (0.95–1.05) were screened by a cDNA dilution series (S4 Table). Quantification of
566 gene expression level was performed with TB Green™ Premix Ex Taq™ Tli RNase H Plus (Takara) on a
567 LightCycler 480 system (Roche). Target genes expression was normalized by the commonly used
568 housekeeping gene *actin5c* (GenBank: AJ862721.1) and calculated using the $2^{-\Delta\Delta Ct}$ method. Each treatment
569 contained four biological replicates and technical triplicates.
570

571 **Identification of *BgElo* gene family members**

572 Both BLASTN and BLASTP were used to search *BgElo* genes in *B. germanica* genome data [57] and
573 our own full-length transcriptome data (NCBI accessions: SRR9143014 and SRR9143013) using the
574 homologous genes of *Elongase* from *D. melanogaster* as query sequences. Candidate *BgElo* genes were
575 amplified with the PrimeSTAR GXL DNA Polymerase reagent (Takara) (primers are listed in S4 Table), the
576 amplified fragments were inserted into the pMD™ 19-T Vector (Takara) and re-sequenced. Candidate *BgElo*
577 genes were then translated and submitted to SMART online tools (http://smart.embl-heidelberg.de) to
578 analyze the conserved structures; only genes with the typical ELO domain were confirmed as *BgElo* genes.
579 The putative *BgElo* mRNA sequences were mapped to the genomic data (GenBank: PYGN00000000.1)
580 using a local BLASTN tool, and the intron-exon structure was analyzed based on the GT-AG rule. The
581 conservative motifs in *BgElos* were analyzed by sequence alignment with DNAMAN 9.0 software.
582

583 **Expression profile analysis**

584 In order to screen the potential *BgElo* genes involved in HC biosynthesis, the expression levels of
585 different *BgElo* genes were quantified in the fat body and abdominal integument, where HCs or their
586 precursors were generated. In addition, other tissues including the head, thorax, gut, legs, ovaries, Malpighian
587 tubules, ejaculatory duct (from two-day-old males), and colleterial glands were dissected from two-day-old
588 females, and were used to analyze the expression profiles of *BgElo12* and *BgElo24* among different tissues.
589 In order to study the time course of *BgElo12*, *BgElo24*, *BgDTra*, and *BgDsx* transcript levels during sexual
590 maturation, a representative nymphal stage (4-day-old sixth-instar nymph, N6D4) and AD0–AD6 females
591 and males were collected. Total RNA was extracted from various tissues or intact cockroaches, and the
592 expression profiles of different genes were studied *via* RT-qPCR.
593

594 **Transcript knockdown *via* RNAi**

595 Gene-specific target sequences as well as a heterologous fragment from *Mus musculus* (*Muslta*) used
596 for double-stranded RNA (dsRNA) synthesis were amplified and cloned into pMD^{TM} 19-T Vector (Takara).
597 Templates used for single-stranded RNA were amplified with primers that incorporated with the T7 promoter
598 sequence (S4 Table). Different kinds of dsRNA were subsequently generated with the T7 RiboMAX™
599 Express RNAi System (Promega). Delivery of dsRNA was performed with a Nanoject II micro-injector
600 (Drummond Scientific) for fourth-instar cockroaches and microliter syringes for fifth-, sixth-instar, and adult
601 cockroaches. For RNAi screen of *BgElo* genes in HC biogenesis, a double injection strategy was employed:
602 the first injection was performed at the early fifth-instar (1- or 2-day-old fifth-instar, N5D1-N5D2) with a
603 dosage of 3 μg in 2 μL; the second injection was performed one week later with a dosage of 4 μg in 2 μL.
604 For confirming the function of *BgElo12* in contact sex pheromone biosynthesis, a third injection with 4 μg
605 of dsRNA in 2 μL was carried out on 1-day-old adults (AD1), and methyl ketones were extracted at AD6.
606 Knockdown of sex-determination genes was accomplished with three dsRNA injections, the first at early
607 fourth instar (N4D1-N4D2), the second at early fifth instar (N5D1-N5D2), and the last at early sixth instar
608 (N6D1-N6D2). The fourth-instar cockroaches were injected with ~0.5 μg of dsRNA in ~0.2 μL; the fifth-
609 and sixth-instar cockroaches were injected with 1 μg of dsRNA in 2 μL. In order to verify the function of
610 *BgElo12* and *BgElo24* in HC biosynthesis and sex-determination genes in modulating *BgElo12* mRNA levels
611 or HC profiles, two non-overlapping gene-specific targets were designed and used in this study, as there are
612 some isoforms of *BgDsx* and *BgTra*, the RNAi targets were designed within the common sequence region.

613

614 **Heterologous expression and fatty acid analysis**

615 Heterologous expression was performed as described [86]. Complete coding sequences (CDS) of
616 *BgElo12*, *BgElo24*, or control (*GFP*) were amplified with PrimeSTAR® HS DNA Polymerase (Takara) using
617 gene-specific primers (S4 Table) that contain the restriction enzyme sites (*KpnI* and *BamHI* for *BgElo12* and
618 *BgElo24*; *BmHI* and *EcoRI* for *GFP*) and the yeast consensus sequence (TACACA) following the restriction
619 enzyme sites (only for forward primers). The amplified *BgElo12*, *BgElo24*, or *GFP* CDS fragments were
620 ligated into the linearized pYES2 shuttle plasmid (Thermo Fisher Scientific) and verified by sequencing. The
621 recombinant plasmids were transformed into INVSc1 *Saccharomyces cerevisiae* (Thermo Fisher Scientific)
622 using the PEG-LiAc method, and streaked onto *S. cerevisiae* minimal medium minus uracil (SC-Uracil)
623 plates to select transformants; single colonies were inoculated in SC-Uracil medium with 2% glucose. After
624 culturing at 30°C for 24 h, the yeast was collected and diluted to an OD600 of 0.4 with SC–Uracil medium
625 containing 1% raffinose and 2% galactose, and further cultured at 30°C until they reached an OD600 of 0.8.
626 At this point, transcription of exogenous genes was examined by RT-PCR. Substrates of C20 (0.5 mM), C22
627 (1 mM), C24 (1 mM), C26 (1 mM), C28 (1 mM), 2-methylhexadecanoic acid (0.5 mM), and 14-
628 methylhexadecanoic acid (0.5 mM) were separately added into the cultures with an extra 1% of tergitol type
629 Nonidet P-40. All the substrates were purchased from Sigma-Aldrich (Louis, MO, USA) or TCI (Shanghai,
630 China).

631 After 48 h, yeast cells were harvested by centrifugation at 500 g for 5 min and washed thrice with Hank's
632 balanced salt solution for fatty acid derivatization and analysis. Pellets were dried under a steam of nitrogen
633 and 2 mL of 1% (v/v) H_2SO_4 in methanol was added, the mixture was vortexed and incubated at 80°C in a
634 N_2 atmosphere for 2 h [87]. After that, 1 ml of saturated sodium chloride solution was added into the mixture
635 and FAMEs were extracted with 1 mL of hexane three times. The FAME extracts were concentrated and
636 subjected to GC–MS analysis as described above. Different FAMEs were identified by comparison to FAME
637 standards (purchased from Sigma-Aldrich) and their mass spectra.

638

639 **Desiccation bioassay**

640 The capacity of *BgElo12* and *BgElo24* to contribute to water retention was assessed by a desiccation
641 bioassay. Drying bottles were prepared by putting ~120 g of packed fresh silica gel into a ~900 mL sealed

642 plastic bottle. The RH inside the bottle dropped to 5% within 2 h which was monitored by HOBO Pro v2
643 (Onset, Bourne, USA). AD2 females were injected with ds*BgElo12*, ds*BgELo24*, and ds*Muslta* and
644 separately caged in the desiccation bottles at 30°C, supplied with ~1 g of dry food, but no water. Survival
645 was recorded every 8 h until all the cockroaches died. About 100 cockroaches were used for each treatment.
646

647 **Courtship behavioral study**

648 Courtship behavior was tested as described [88]. Antennae from differently treated AD3 or AD5 females
649 were excised, and each antenna was attached to the tip of a glass Pasteur pipette with paraffin, the antenna
650 was used immediately to test the responses of AD13–15 males that were separated from females since
651 eclosion. The test antenna was used to touch the antennae of the male, and a positive response was recorded
652 if the male cockroach turned its body and raised the wings to approximately 90 degrees within 30 sec. A
653 negative response was recorded if the test antenna failed to elicit a response in a male cockroach and this
654 male then responded to a positive control antenna from a normal AD6 female. The wing raising (WR) latency
655 was recorded according to Wada-Katsumata and Schal [61]; the latency of the WR display was timed from
656 contact of the antennae to the initiation of the male WR display. All female antennae and male cockroaches
657 were used only once, all tests were performed in the scotophase and we avoided the first and last 2 h of the
658 scotophase. Bioassays were conducted under a dim red light to simulate a dark environment.
659

660 **Dual-luciferase reporter gene assay**

661 The 5' end of *BgElo12* was obtained by 5' Rapid Amplification of cDNA Ends (RACE). 5' RACE
662 cDNA library was prepared using Clontech SMARTer RACE 5'/3' Kit (Takara) according to the user manual
663 with the gene-specific primer (S4 Table) and kit-provided Universal long primer. The amplified fragments
664 were cloned into pRACE vector and sequenced. About a 2.7 kb sequence upstream of *BgElo12* was amplified
665 and cloned into pGL3-basic vector, and the CDS sequences of $BgDsx^{M}$ and GFP (control) were separately
666 cloned into the expression vector pCDNA3.1. The HEK293T cells were cultured in a 24-well plate with 500
667 μL of DMEM medium (Thermo Fisher Scientific) for 24 h before transfection, and the restructured pGL3-
668 basic vector (200 ng/well) was co-transfected with the expression vectors (200 ng/well) to HEK293T cells
669 using Lipofectamine™ 3000 (Invitrogen, Carlsbad, CA, USA). The pRL-TK that encoded a *Renilla*
670 luciferase was also co-transfected as an internal control. The transfected cells were cultured at 37°C for 36 h

671 and subjected to luciferase activity analysis using the Dual-Glo Luciferase Assay System (Promega, Madison,
672 WI, USA).
673

674 **Statistics**

675 Data were statistically analyzed using SPSS 23 and presented as mean ± SEM or mean ± SD.
676 Two-tailed Student's *t*-test was used for two-group comparison; significant differences between multi-groups
677 were analyzed by one-way ANOVA followed by the LSD test (Equal variances assumed) or Welch's
678 ANOVA followed by Games-Howell multiple comparisons test (Equal variances not assumed) at $P < 0.05$
679 level. Principal component analysis (PCA) was used to distinguish the CHC profiles of AD1 and AD6
680 cockroaches.
681

682 **Data availability**

683 PacBio data sets have been deposited in NCBI's SRA under the accession numbers SRR9143014 and
684 SRR9143013. All *BgElo* sequences have been submitted to NCBI's GenBank under the accession numbers
685 MT925720 and MW380216–MW380238
686

687 ## Acknowledgments

688 We thank Shang-Wang Hong from Northwest A & F University for his help in sequence analysis, and we
689 also express our specially thanks to Hao-Su Cong and Henry Chung from Michigan State University for their
690 valuable suggestions.
691

692 ## Author contributions

693 **Conceptualization:** Xiao-Jin Pei, Yong-Liang Fan.
694 **Funding acquisition:** Yong-Liang Fan, Coby Schal, Tong-Xian Liu.
695 **Investigation:** Xiao-Jin Pei, Yu Bai, Tian-Tian Bai, Zhan-Feng Zhang, Nan Chen.
696 **Methodology:** Xiao-Jin Pei, Yu Bai, Zhan-Feng Zhang, Nan Chen.
697 **Project administration:** Yong-Liang Fan, Coby Schal, Tong-Xian Liu.

698 **Resources:** Yong-Liang Fan, Coby Schal, Sheng Li, Tong-Xian Liu.

699 **Supervision:** Yong-Liang Fan, Tong-Xian Liu.

700 **Writing – original draft:** Xiao-Jin Pei.

701 **Writing – review & editing:** Xiao-Jin Pei, Yong-Liang Fan, Yu Bai, Tian-Tian Bai, Coby Schal, Zhan-Feng
702 Zhang, Nan Chen, Sheng Li, Tong-Xian Liu.

703

704 References

705 1. Bear A, Monteiro A. Both cell-autonomous mechanisms and hormones contribute to sexual
706 development in vertebrates and insects. BioEssays. 2013; 35:725–732.
707 https://doi.org/10.1002/bies.201300009.
708 2. Darwin C. 1871. The descent of man, and selection in relation to sex. London, UK: J. Murray.
709 3. Andersson M. Sexual selection. Princeton, NJ: Princeton University Press; 1994.
710 4. Connallon T, Knowles LL. Intergenomic conflict revealed by patterns of sex-biased gene expression.
711 Trends Genet. 2005; 21:495–499. https://doi.org/10.1016/j.tig.2005.07.006.
712 5. Innocenti P, Morrow EH. The sexually antagonistic genes of *Drosophila melanogaster*. PLoS Biol.
713 2010; 8:e1000335. https://doi.org/10.1371/journal.pbio.1000335.
714 6. Mank JE. The transcriptional architecture of phenotypic dimorphism. Nature Ecol Evol. 2017; 1:6.
715 https://doi.org/10.1038/s41559-016-0006.
716 7. Rogers TF, Palmer DH, Wright AE. Sex-specific selection drives the evolution of alternative splicing in
717 birds. Mol Biol Evol. 2021; 38:519–530. https://doi.org/10.1093/molbev/msaa242.
718 8. 8. Kopp A. *Dmrt* genes in the development and evolution of sexual dimorphism. Trends Genet. 2012;
719 28:175–184. https://doi.org/10.1016/j.tig.2012.02.002.
720 9. Williams TM, Selegue JE, Werner T, Gompel N, Kopp A, Carroll SB. The regulation and evolution of a
721 genetic switch controlling sexually dimorphic traits in *Drosophila*. Cell. 2008; 134:610–623.
722 https://doi.org/10.1016/j.cell.2008.06.052.
723 10. Tanaka K, Barmina O, Sanders LE, Arbeitman MN, Kopp A. Evolution of sex-specific traits through
724 changes in HOX-dependent *doublesex* expression. PLoS Biol. 2011; 9:e1001131.
725 https://doi.org/10.1371/journal.pbio.1001131.

11. Clough E, Jimenez E, Kim YA, Whitworth C, Neville MC, Hempel LU, et al. Sex- and tissue-specific functions of *Drosophila* doublesex transcription factor target genes. Dev Cell. 2014; 31:761–773. https://doi.org/10.1016/j.devcel.2014.11.021.
12. Prakash A, Monteiro A. Molecular mechanisms of secondary sexual trait development in insects. Curr Opin Insect Sci. 2016; 17:40–48. https://doi.org/10.1016/j.cois.2016.06.003.
13. Hasselmann M, Gempe T, Schiøtt M, Nunes-Silva CG, Otte M, Beye M. Evidence for the evolutionary nascence of a novel sex determination pathway in honeybees. Nature. 2008; 454:519–522. https://doi.org/10.1038/nature07052.
14. Zhang Z, Klein J, Nei M. Evolution of the *sex-lethal* gene in insects and origin of the sex-determination system in *Drosophila*. J Mol Evol. 2014; 78:50–65. https://doi.org/10.1007/s00239-013-9599-3.
15. Kiuchi T, Koga H, Kawamoto M, Shoji K, Sakai H, Arai Y, et al. A single female-specific piRNA is the primary determiner of sex in the silkworm. Nature. 2014; 509:633–636. https://doi.org/10.1038/nature13315.
16. Herpin A, Schartl M. Plasticity of gene-regulatory networks controlling sex determination: of masters, slaves, usual suspects, newcomers, and usurpators. EMBO Rep. 2015; 16:1260–1274. https://doi.org/10.15252/embr.201540667.
17. Hall AB, Basu S, Jiang X, Qi Y, Timoshevskiy VA, Biedler JK, et al. A male-determining factor in the mosquito *Aedes aegypti*. Science. 2015; 348:1268–1270. https://doi.org/10.1126/science.aaa2850.
18. Gibbs AG. Water-proofing properties of cuticular lipids. Am Zool. 1998; 38:471–482. https://doi.org/10.1093/icb/38.3.471.
19. Blomquist GJ, Ginzel MD. Chemical ecology, biochemistry, and molecular biology of insect hydrocarbons. Annu Rev Entomol. 2021; 66:45–60. https://doi.org/10.1146/annurev-ento-031620-071754.
20. Howard RW, Blomquist GJ. Ecological, behavioral, and biochemical aspects of insect hydrocarbons. Annu Rev Entomol. 2005; 50:371–393. https://doi.org/10.1146/annurev.ento.50.071803.130359.
21. Ingleby FC, Innocenti P, Rundle HD, Morrow EH. Between-sex genetic covariance constrains the evolution of sexual dimorphism in *Drosophila melanogaster*. J Evol Biol. 2014; 27:1721–1732. https://doi.org/10.1111/jeb.12429.

22. Zhang B, Xue HJ, Song KQ, Liu J, Li WZ, Nie RE, et al. Male mate recognition via cuticular hydrocarbons facilitates sexual isolation between sympatric leaf beetle sister species. J Insect Physiol. 2014; 70:15–21. https://doi.org/10.1016/j.jinsphys.2014.08.006.
23. Berson JD, Garcia-Gonzalez F, Simmons LW. Experimental evidence for the role of sexual selection in the evolution of cuticular hydrocarbons in the dung beetle, *Onthophagus taurus*. J Evol Biol. 2019; 32:1186–1193. https://doi.org/10.1111/jeb.13519.
24. Juárez MP, Ayala S, Brenner RR. Methyl-branched fatty acid biosynthesis in *Triatoma infestans*. Insect Biochem Mol Biol. 1996; 26:599–605. https://doi.org/10.1016/S0965-1748(96)00021-5.
25. Juárez MP, Chase J, Blomquist GJ. A microsomal fatty acid synthetase from the integument of *Blattella germanica* synthesizes methyl-branched fatty acids, precursors to hydrocarbon and contact sex pheromone. Arch Insect Biochem Physiol. 1992; 293:333–341. https://doi.org/10.1016/0003-9861(92)90403-j.
26. Blomquist GJ, Tillman JA, Reed JR, Gu P, Vanderwel D, Choi S, et al. Regulation of enzymatic activity involved in sex pheromone production in the housefly, *Musca domestica*. Insect Biochem Mol Biol. 1995; 25:751–757. https://doi.org/10.1016/0965-1748(95)00015-n.
27. Parvy JP, Napal L, Rubin T, Poidevin M, Perrin L, Wicker-Thomas C, et al. *Drosophila melanogaster* Acetyl-CoA-carboxylase sustains a fatty acid-dependent remote signal to waterproof the respiratory system. PLoS Genets. 2012; 8:e1002925. https://doi.org/10.1371/journal.pgen.1002925.
28. Chung H, Loehlin DW, Dufour HD, Vaccarro K, Millar JG, Carroll SB. A single gene affects both ecological divergence and mate choice in *Drosophila*. Science. 2014; 343:1148–1151. https://doi.org/10.1126/science.1249998.
29. Wicker-Thomas C, Garrido D, Bontonou G, Napal L, Mazuras N, Denis B, et al. Flexible origin of hydrocarbon/pheromone precursors in *Drosophila melanogaster*. J Lipid Res. 2015; 56:2094–2101. https://doi.org/10.1194/jlr.M060368.
30. Ginzel MD, Blomquist GJ. Insect hydrocarbons: biochemistry and chemical ecology. In: Cohen E, Moussian B, editors. Extracellular Composite Matrices in Arthropods. Springer; 2016. pp. 221–252.
31. Chertemps T, Duportets L, Labeur C, Ueyama M, Wicker-Thomas C. A female specific desaturase gene responsible for diene hydrocarbon biosynthesis and courtship behaviour in *Drosophila melanogaster*. Insect Mol Biol. 2006; 15:465–473. https://doi.org/10.1111/j.1365-2583.2006.00658.x.

32. Legendre A, Miao XX, Da Lage JL, Wicker-Thomas C. Evolution of a desaturase involved in female pheromonal cuticular hydrocarbon biosynthesis and courtship behavior in *Drosophila*. Insect Biochem Mol Biol. 2008; 38:244–255. https://doi.org/10.1016/j.ibmb.2007.11.005.
33. Chertemps T, Duportets L, Labeur C, Ueda R, Takahashi K, Saigo K, et al. A female-biased expressed elongase involved in long-chain hydrocarbon biosynthesis and courtship behavior in *Drosophila melanogaster*. Proc Natl Acad Sci USA. 2007; 104: 4273–4278. https://doi.org/10.1073/pnas.0608142104.
34. Qiu Y, Tittiger C, Wicker-thomas C, Goff LG, Young S, Wajnberg E, et al. An insect-specific p450 oxidative decarbonylase for cuticular hydrocarbon biosynthesis. Proc Natl Acad Sci USA. 2012; 109:14858–14863. https://doi.org/10.1073/pnas.1208650109.
35. MacLean M, Nadeau J, Gurnea T, Tittiger C, Blomquist GJ. Mountain pine beetle (*Dendroctonus ponderosae*) *CYP4Gs* convert long and short chain alcohols and aldehydes to hydrocarbons. Insect Biochem Mol Biol. 2018; 102:11–20. https://doi.org/10.1016/j.ibmb.2018.09.005.
36. Li DT, Chen X, Wang XQ, Zhang CX. *FAR* gene enables the brown planthopper to walk and jump on water in paddy field. Sci China Life Sci. 2019; 62:1521–1531. https://doi.org/10.1007/s11427-018-9462-4.
37. Blomquist GJ, Bagnères AG. Insect hydrocarbons: biology, biochemistry, and chemical ecology. 1st ed. New York: Cambridge University Press; 2010.
38. Chung H, Carroll SB. Wax, sex and the origin of species: Dual roles of insect cuticular hydrocarbons in adaptation and mating. BioEssays. 2015; 37:822–830. https://doi.org/10.1002/bies.201500014.
39. Holze H, Schrader L, Buellesbach J. Advances in deciphering the genetic basis of insect cuticular hydrocarbon biosynthesis and variation. Heredity. 2021; 126:219–234. https://doi.org/10.1038/s41437-020-00380-y.
40. Ferveur JF, Sureau G. Simultaneous influence on male courtship of stimulatory and inhibitory pheromones produced by live sex-mosaic *Drosophila melanogaster*. Proc R Soc B. 1996; 263:967–973. https://doi.org/10.1098/rspb.1996.0143.
41. Ferveur JF, Savarit F, O'Kane CJ, Sureau G, Greenspan RJ, et al. Genetic feminization of pheromones and its behavioral consequences in *Drosophila* males. Science. 1997; 276:1555–1558. https://doi.org/10.1126/science.276.5318.1555.

42. Shirangi TR, Dufour HD, Williams TM, Carroll SB. Rapid evolution of sex pheromone-producing enzyme expression in *Drosophila*. PLoS Biol. 2009; 7:e1000168. https://doi.org/10.1371/journal.pbio.1000168.
43. Schal C. Cockroaches. In: Hedges S, Moreland D, editors, Handbook of Pest Control. Pennsylvania State University: GIEMedia; 2011. pp. 150–291.
44. Chase J, Jurenka RA, Schal C, Halarnkar PP, Blomquist GJ. Biosynthesis of methyl branched hydrocarbons of the German cockroach *Blattella germanica* (L.) (Orthoptera, Blattellidae). Insect Biochem. 1990; 20:149-156. https://doi.org/10.1016/0020-1790(90)90007-H.
45. Schal C, Gu X, Burns EL, Blomquist GJ. Patterns of biosynthesis and accumulation of hydrocarbons and contact sex pheromone in the female German cockroach, *Blattella germanica*. Arch Insect Biochem Physiol. 1994; 25:375–391. https://doi.org/10.1002/arch.940250411.
46. Juárez MP. Fatty acyl-CoA elongation in *Blatella germanica* integumental microsomes. Arch Insect Biochem Physiol. 2004; 56: 170–178. https://doi.org/10.1002/arch.20007.
47. Young HP, Larabee JK, Gibbs AG, Schal C. Relationship between tissue-specific hydrocarbon profiles and lipid melting temperatures in the cockroach *Blattella germanica*. J Chem Ecol. 2000; 26:1245-1263. https://doi.org/10.1023/A:1005440212538.
48. Chase J, Touhara K, Prestwich GD, Schal C, Blomquist GJ. Biosynthesis and endocrine control of the production of the German cockroach sex pheromone 3,11-dimethylnonacosan-2-one. Proc Natl Acad Sci USA. 1992; 89:6050–6054. https://doi.org/10.1073/pnas.89.13.6050.
49. Nojima S, Nishida R, Kuwahara Y, Sakuma M. Nuptial feeding stimulants: a male courtship pheromone of the German cockroach, *Blattella germanica* (L.) (Dictyoptera: Blattellidae). Naturwissenschaften. 1999; 86:193-196. https://doi.org/10.1007/s001140050596.
50. Eliyahu D, Nojima S, Mori K, Schal C. New contact sex pheromone components of the German cockroach, *Blattella germanica*, predicted from the proposed biosynthetic pathway. J Chem Ecol. 2008; 34:229–237. https://doi.org/10.1007/s10886-007-9409-8.
51. Eliyahu D, Nojima S, Mori K, Schal C. Jail baits: how and why nymphs mimic adult females of the German cockroach, *Blattella germanica*. Anim Behav. 2009; 78:1097–1105. https://doi.org/10.1016/j.anbehav.2009.06.035.
52. Wexler J, Delaney EK, Belles X, Schal C, Wada-Katsumata A, et al. Hemimetabolous insects elucidate

842 the origin of sexual development via alternative splicing. eLife. 2019; 8:e47490.
843 https://doi.org/10.7554/eLife.47490.
844 53. Schal C, Chiang AS. Hormonal control of sexual receptivity in cockroaches. Experientia. 1995;
845 51:994–998. https://doi.org/10.1007/BF01921755.
846 54. Jurenka RA, Schal C, Burns E, Chase J, Blomquist GJ. Structural correlation between cuticular
847 hydrocarbons and female contact sex pheromone of German cockroach *Blattella germanica* (L.). J
848 Chem Ecol. 1989; 15:939–949. https://doi.org/10.1007/BF01015189.
849 55. Pei XJ, Chen N, Bai Y, Qiao JW, Li S, et al. *BgFas1*: A fatty acid synthase gene required for both
850 hydrocarbon and cuticular fatty acid biosynthesis in the German cockroach, *Blattella germanica* (L.).
851 Insect Biochem Mol Biol. 2019; 112:103203. https://doi.org/10.1016/j.ibmb.2019.103203.
852 56. Chen N, Pei XJ, Li S, Fan YL, Liu TX. Involvement of integument-rich *CYP4G19* in hydrocarbon
853 biosynthesis and cuticular penetration resistance in *Blattella germanica* (L.). Pest Manag Sci. 2020;
854 76:215–226. https://doi.org/10.1002/ps.5499.
855 57. Harrison MC, Jongepier E, Robertson HM, Arning N, Bitard-Feildel T, Chao H, et al. Hemimetabolous
856 genomes reveal molecular basis of termite eusociality. Nat Ecol Evol. 2018; 2:557–566.
857 https://doi.org/10.1038/s41559-017-0459-1.
858 58. Moon YA, Shah NA, Mohapatra S, Warrington JA, Horton JD. Identification of a mammalian long
859 chain fatty acyl elongase regulated by sterol regulatory element-binding proteins. J Biol Chem. 2001;
860 276:45358–45366. https://doi.org/10.1074/jbc.M108413200.
861 59. Toke DA, Martin CE. Isolation and characterization of gene affecting fatty acid elongation in
862 *Saccharomyces cerevisiae*. J Biol Chem. 1996; 271:18413–18422.
863 https://doi.org/10.1074/jbc.271.31.18413.
864 60. Oh CS, Toke DA, Mandala S, Martin CE. *ELO2* and *ELO3*, Homologues of the *Saccharomyces*
865 *cerevisiae ELO1* gene, function in fatty acid elongation and are required for sphingolipid formation. J
866 Boil Chem. 1997; 272:17376–17384. https://doi.org/10.1074/jbc.272.28.17376.
867 61. Wada-Katsumata A, Schal C. Antennal grooming facilitates courtship performance in a group-living
868 insect, the German cockroach *Blattella germanica*. Sci Rep. 2019; 9:2942.
869 https://doi.org/10.1038/s41598-019-39868-x.
870 62. Schal C, Burns EL, Jurenka RA, Blomquist GJ. A new component of the female sex pheromone of

871 *Blattella germanica* (L.) (Dictyoptera: Blattellidae) and interaction with other pheromone components.
872 J Chem Ecol. 1990; 16:1997–2008. https://doi.org/10.1007/BF01020511.
873 63. Gu X, Quilici D, Juarez P, Blomquist GJ, Schal C. Biosynthesis of hydrocarbons and contact sex
874 pheromone and their transport by lipophorin in females of the German cockroach (*Blattella*
875 *germanica*). J Insect Physiol. 1995; 41:257–267. https://doi.org/10.1016/0022-1910(94)00100-U.
876 64. Ohno Y, Suto S, Yamanaka M, Mizutani Y, Mitsutake S, Igarashi Y, et al. ELOVL1 production of C24
877 acyl-CoAs is linked to C24 sphingolipid synthesis. Proc Natl Acad Sci USA. 2010; 107:18439–18444.
878 https://doi.org/10.1073/pnas.1005572107.
879 65. Pfannenstiel RS, Booth W, Vargo EL, Schal C. *Blattella asahinai* (Dictyoptera: Blattellidae): A new
880 predator of lepidopteran eggs in south Texas soybean. Ann Entomol Soc Am. 2008; 101:763–768.
881 66. Schal C, Sevala V, Capurro ML, Snyder TE, Blomquist GJ, Bagnères AG. Tissue distribution and
882 lipophorin transport of hydrocarbons and sex pheromones in the house fly, *Musca domestica*. J Insect
883 Sci. 2001; 1:12.
884 67. Schal C, Sevala V, Cardé RT. Novel and highly specific transport of a volatile sex pheromone by
885 hemolymph lipophorin in moths. Naturwissenschaften. 1998; 85: 339–342.
886 https://doi:10.1007/s001140050511.
887 68. Li DT, Chen X, Wang XQ, Moussian, B, Zhang CX. The fatty acid elongase gene family in the brown
888 planthopper, *Nilaparvata lugens*. Insect Biochem Mol Biol. 2019; 108:32–43.
889 https://doi.org/10.1016/j.ibmb.2019.03.005.
890 69. Zhao X, Yang Y, Niu N, Zhao Y, Zhang J. The fatty acid elongase gene *LmElo7* is required for
891 hydrocarbon biosynthesis and cuticle permeability in the migratory locust, *Locusta migratoria*. J Insect
892 Physiol. 2020; 123: 104052. https://doi.org/10.1016/j.jinsphys.2020.104052.
893 70. Gempe T, Beye M. Function and evolution of sex determination mechanisms, genes and pathways in
894 insects. BioEssays. 2011; 33:52–60. https://doi.org/10.1002/bies.201000043.
895 71. Verhulst EC, van de Zande L. Double nexus–*Doublesex* is the connecting element in sex determination.
896 Brief Funct Genomics. 2015; 14:396–406. https://doi.org/10.1093/bfgp/elv005.
897 72. Wicker C, Jallon JM. Hormonal control of sex pheromone biosynthesis in *Drosophila melanogaster*. J
898 Insect Physiol. 1995; 41:65–70. https://doi.org/10.1016/0022-1910(94)00074-Q.
899 73. Wicker C, Jallon JM. Influence of ovary and ecdysteroids on pheromone biosynthesis in *Drosophila*

900 *melanogaster* (Diptera: Drosophilidae). Eur J Entomol. 1995; 92:197202.
901 74. Marican C, Duportets L, Birman S, Jallon JM. Female-specific regulation of cuticular hydrocarbon
902 biosynthesis by dopamine in *Drosophila melanogaster*. Insect Biochem Mol Biol. 2004; 34:823–830.
903 https://doi.org/10.1016/j.ibmb.2004.05.002.
904 75. Kuo TH, Fedina TY, Hansen I, Dreisewerd K, Dierick HA, Yew JY, et al. Insulin signaling mediates
905 sexual attractiveness in *Drosophila*. PLoS Genet. 2012; 8:e1002684.
906 https://doi.org/10.1371/journal.pgen.1002684.
907 76. Bontonou G, Shaik HA, Denis B, Wicker-Thomas C. Acp70A regulates *Drosophila* pheromones
908 through juvenile hormone induction. Insect Biochem Mol Biol. 2015; 56:36–49.
909 https://doi.org/10.1016/j.ibmb.2014.11.008.
910 77. Fedina TY, Arbuthnott D, Rundle HD, Promislow D, Pletcher SD. Tissue-specific insulin signaling
911 mediates female sexual attractiveness. PLoS Genet. 2017; 13:e1006935.
912 https://doi.org/10.1371/journal.pgen.1006935.
913 78. Baron A, Denis B, Wicker-Thomas C. Control of pheromone production by ovaries in *Drosophila*. J
914 Insect Physiol. 2018; 109:138–143. https://doi.org/10.1016/j.jinsphys.2018.07.003.
915 79. Bownes M, Smith T. Ecdysteroids in adult males and females of *Drosophila melanogaster*. J Insect
916 Physiol. 1984; 30:823–830. https://doi.org/10.1016/0022-1910(84)90019-2.
917 80. Romaá I, Pascual, N, Bellés X. The ovary is a source of circulating ecdysteroids in *Blattella germanica*
918 (Dictyoptera: Blattellidae). Eur J Entomol. 1995; 92:93-103.
919 81. Zinna RA, Gotoh H, Kojima T, Niimi T. Recent advances in understanding the mechanisms of sexually
920 dimorphic plasticity: insights from beetle weapons and future directions. Curr Opin Insect Sci. 2018;
921 25:35–41. https://doi.org/10.1016/j.cois.2017.11.009.
922 82. Lozano J, Belles X. Conserved repressive function of Krüppel homolog 1 on insect metamorphosis in
923 hemimetabolous and holometabolous species. Sci Rep. 2011; 1:163. https://doi.org/10.1038/srep00163.
924 83. Kunte K. Mimetic butterflies support Wallace's model of sexual dimorphism. Proc R Soc B. 2008;
925 275:1617–1624. https://doi.org/10.1098/rspb.2008.0171.
926 84. 85. Fan YL, Eliyahu D, Schal C. Cuticular hydrocarbons as maternal provisions in embryos and
927 nymphs of the cockroach *Blattella germanica*. J Exp Biol. 2008; 211: 548-554.
928 https://jeb.biologists.org/content/211/4/548.

929 85. Fan YL, Chase J, Sevala VL, Schal C. Lipophorin-facilitated hydrocarbon uptake by oocytes in the
930 German cockroach *Blattella germanica* (L.). J Exp Biol. 2002; 205:781–790.
931 https://jeb.biologists.org/content/205/6/781.
932 86. Hastings N, Agaba M, Tocher DR, Leaver MJ, Dick JR, Sargent JR, et al. A vertebrate fatty acid
933 desaturase with Delta 5 and Delta 6 activities. Proc Natl Acad Sci USA. 2001; 98:14304–14309.
934 https://doi.org/10.1073/pnas.251516598.
935 87. Lepage G, Roy C. Improved recovery of fatty acid through direct transesterification without prior
936 extraction or purification. J Lipid Res. 1984; 25:1391–1396.
937 88. Eliyahu D, Nojima S, Capracotta SS, Comins DL, Schal, C. Identification of cuticular lipids eliciting
938 interspecific courtship in the German cockroach, *Blattella germanica*. Naturwissenschaften. 2008;
939 95:403–412. https://doi.org/10.1007/s00114-007-0339-7.

940 **Support information**

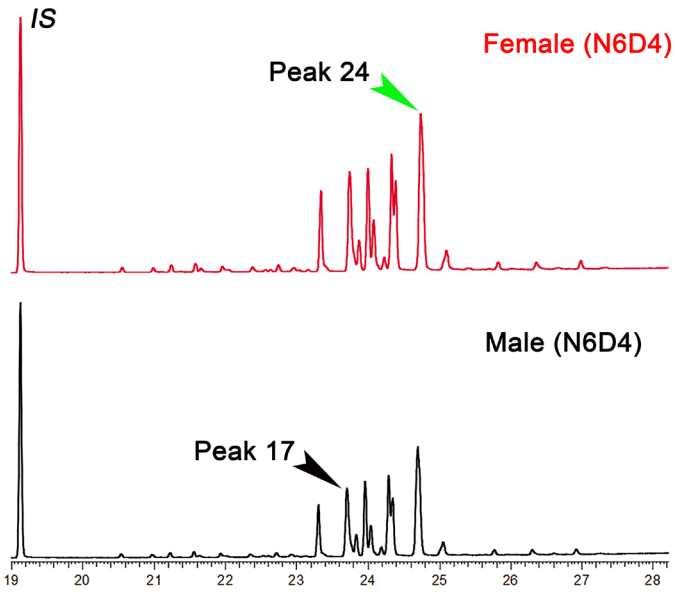

941

942 **S1 Fig.** Cuticular hydrocarbon profiles of 4-day-old sixth-instar nymphs of *Blattella germanica*. Peak 24

943 represents the female-enriched 3,7-; 3,9-; 3,11-DimeC29, and Peak 17 is the male-enriched 9-; 11-; 13-; 15-

944 MeC29.

945

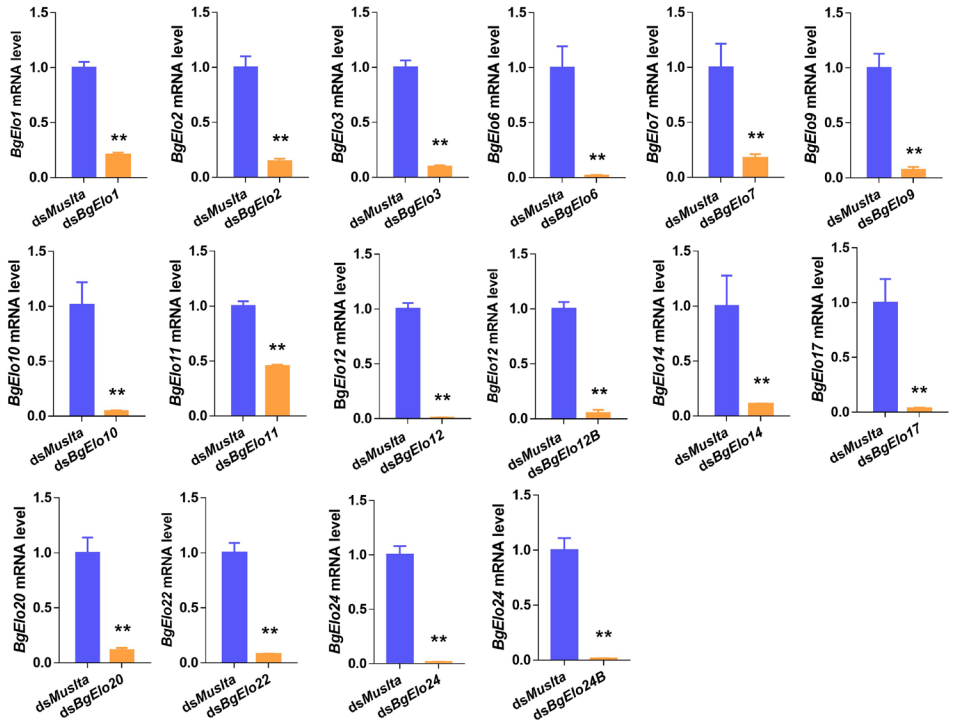

946

947 **S2 Fig**. RNAi efficiency of different *BgElo* genes in *Blattella germanica*. Data are shown as mean ± SEM,

948 calculated from 4 replicates (2–3 cockroaches/replicate); $^{**}P < 0.01$, two-tailed Student's *t*-test.

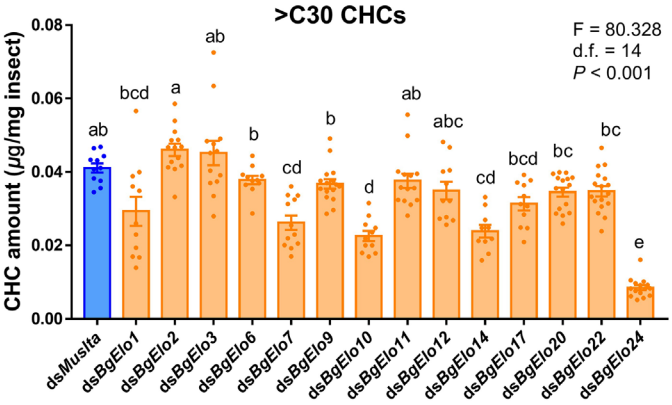

S3 Fig. Effects of *BgElo*-RNAi on cuticular hydrocarbons of *Blattella germanica* with chain length longer than 30. Different letters indicate significant differences between groups using Welch's ANOVA (Games-Howell multiple comparisons test, $P < 0.05$).

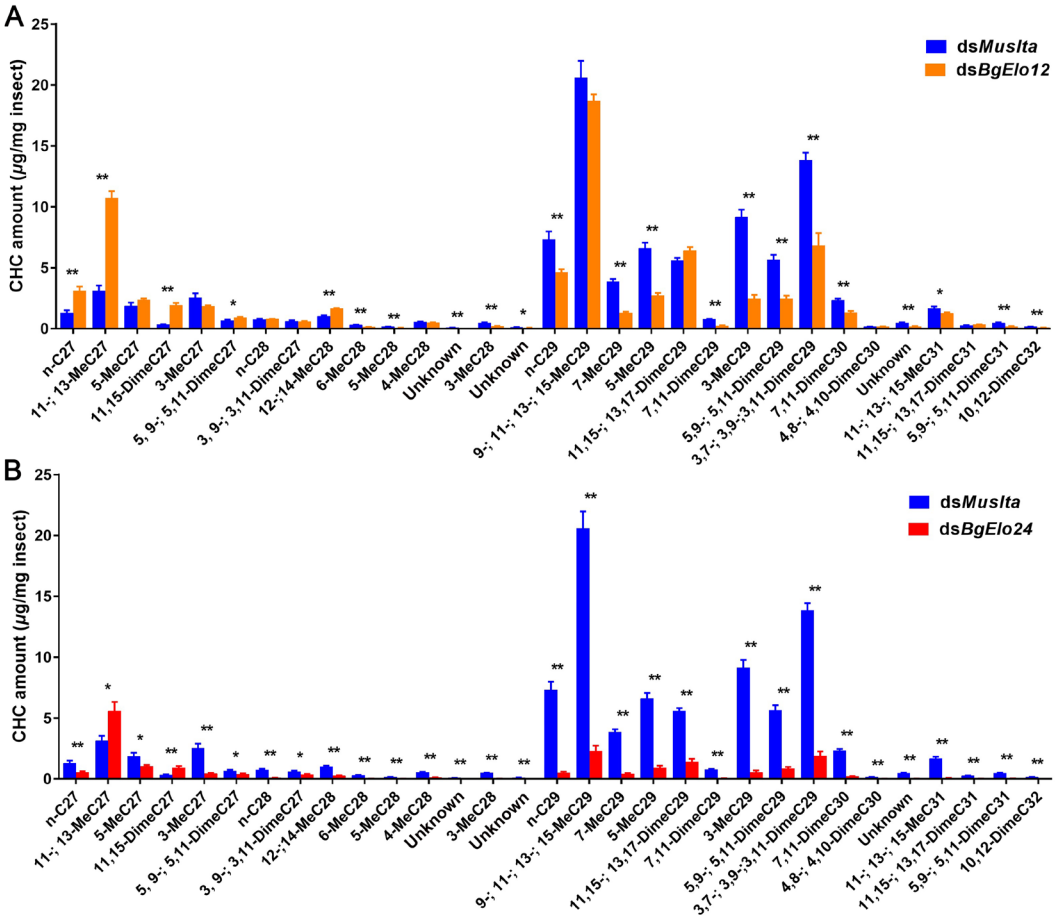

S4 Fig. Effects of *BgElo12*-RNAi and *BgElo24*-RNAi on CHC profiles of male *B. germanica*. Data are shown as mean ± SEM; **P* < 0.05, ***P* < 0.01; two-tailed Student's *t*-test, n = 9 or 10.

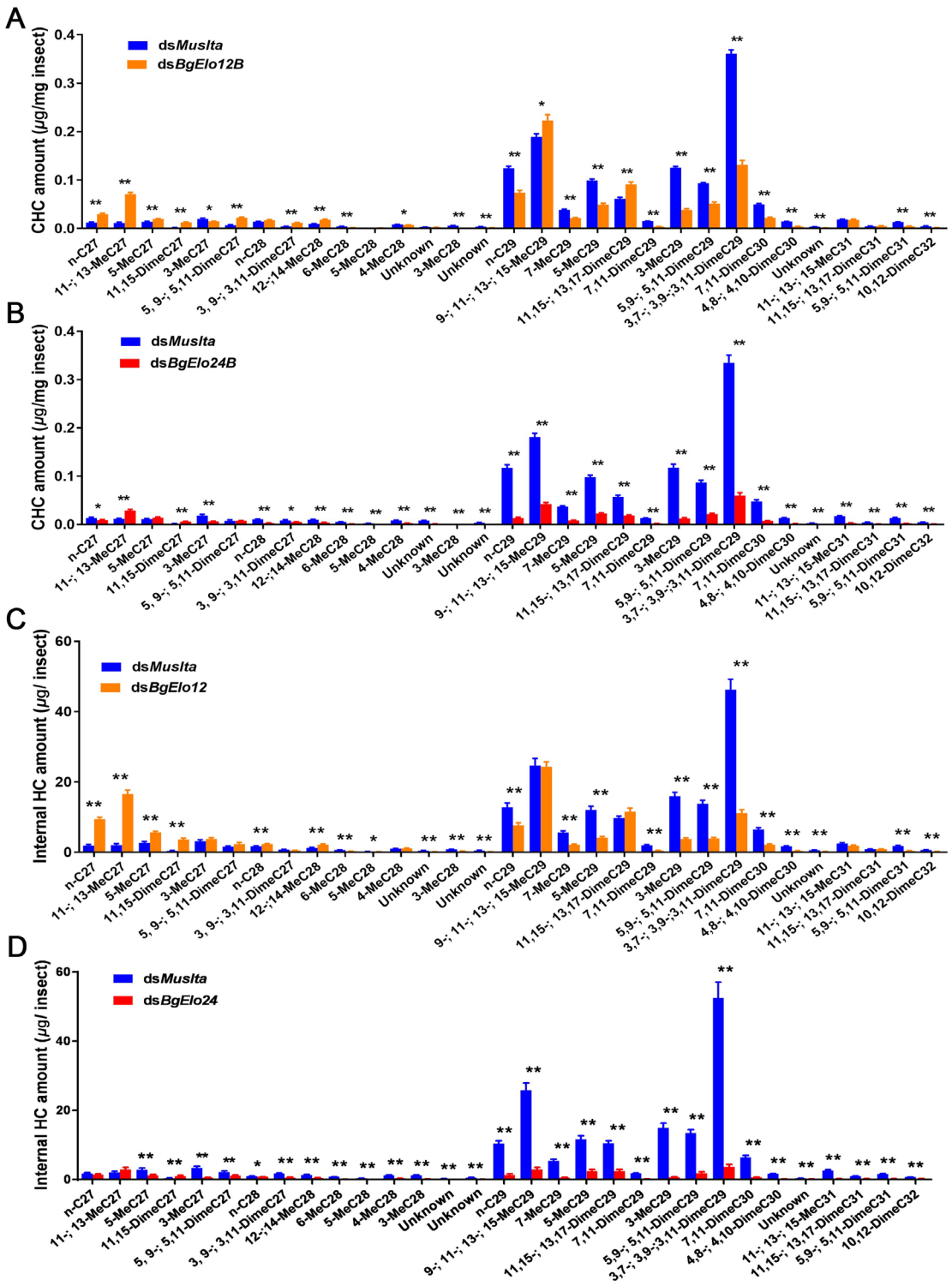

957

958 **S5 Fig**. Verifying the roles of *BgElo12* and *BgElo24* in hydrocarbon biosynthesis by the second RNAi targets.

959 **(A)** Analysis of cuticular hydrocarbons after RNAi of *BgElo12* using the second target (ds*BgElo12B*), **(B)** or

960 after RNAi of *BgElo24* using the second target (ds*BgElo24B*). **(C)** and **(D)** The effects of *BgElo12*-RNAi and

961 *BgElo24*-RNAi on internal hydrocarbons. Data are shown as mean ± SEM; **P* < 0.05, ***P* < 0.01; two-tailed

962 Student's *t*-test, n = 10–12.

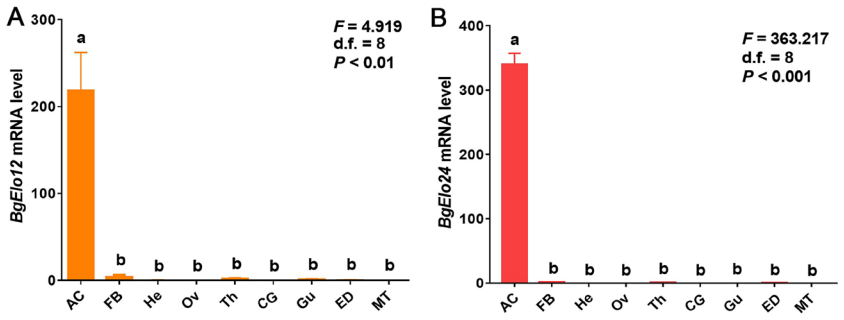

S6 Fig. Tissue-specific expression of *BgElo12* and *BgElo24* in *Blattella germanica*. AC: Abdominal cuticle, FB: Fat body, He: Head, Ov: Ovaries, Th: Thorax, Cg: Colleterial gland, Gu: Gut, ED: Ejaculatory duct, MT: Malpighian tubules. Data are shown as mean ± SEM; and each sample was collected from 4 (AC, Th, Gu), 8 (FB, He, Ov, CG, ED), and 12 (MT) cockroaches. Different letters indicate significant differences between groups using Welch's ANOVA (Games-Howell multiple comparisons test, $P < 0.05$), n = 4.

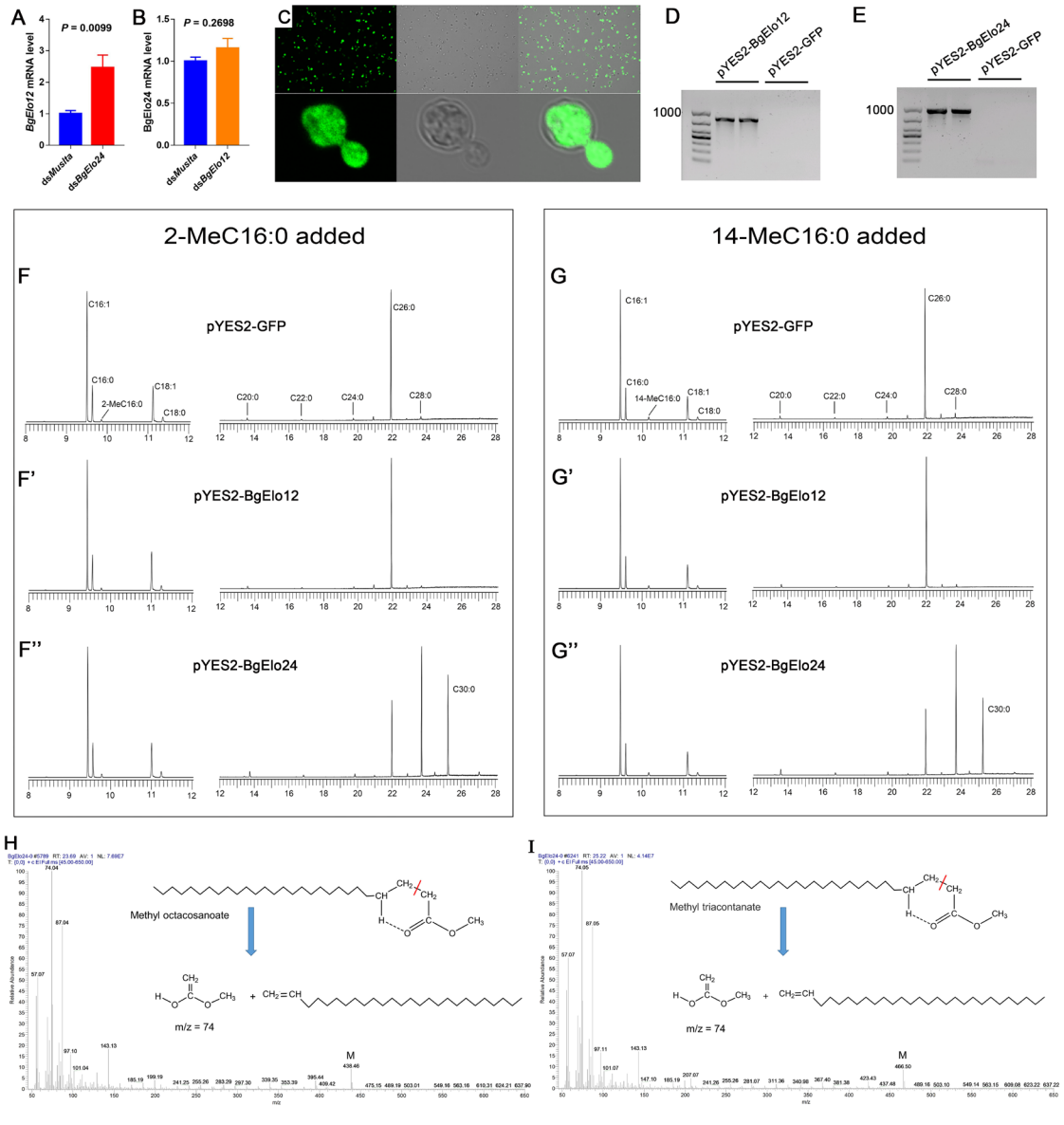

971 **S7 Fig**. Heterologous expression of *BgElo12* and *BgElo24* in yeast. RNAi of *BgElo24* upregulated the
972 expression of *BgElo12* **(A)**, while RNAi of *BgElo12* did not affect *BgElo24* transcript level **(B)**. Data are shown
973 as mean ± SEM; *P* values were calculated from 4 samples; each sample contained 2 cockroaches; two-tailed
974 Student's *t*-test. **(C)** Detection of GFP protein in the yeast with pYES2-GFP using a FV3000 confocal
975 fluorescence microscope (Olympus). **(D)** and **(E)** RT-PCR analysis of the *BgElo12* and *BgElo24* mRNA after the
976 induction with galactose. **(F)**, **(F')**, and **(F'')** Gas chromatograms of fatty acid methyl esters after adding 2-
977 MeC16:0 into the medium. **(G)**, **(G')**, and **(G'')** Gas chromatogram of fatty acid methyl esters after adding 14-
978 MeC16:0 into the medium. The compositions with retention times between 12 and 28 min were magnified about
979 50 times. **(H)** and **(I)** Mass spectra of methyl octacosanoate and methyl triacontanate, both of which showed a
980 strong characteristic ion fragment (m/z = 74) and M peak.
981

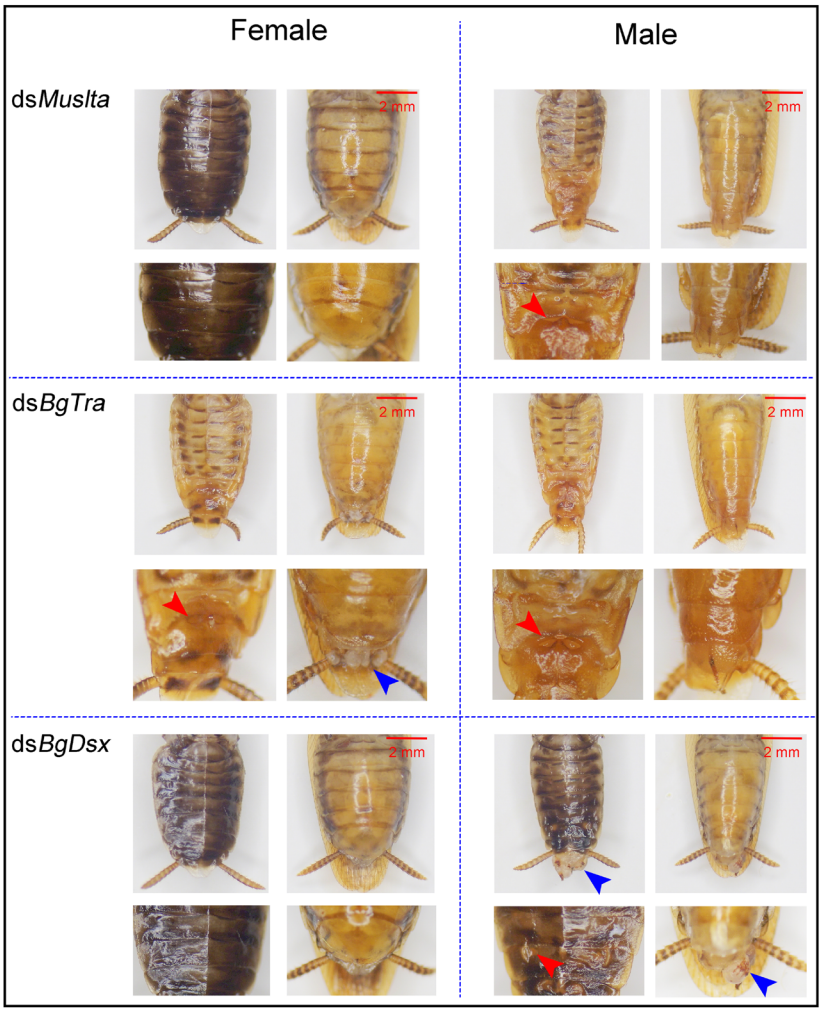

982
983 **S8 Fig**. The sex-specific developmental functions of *BgTra* and *BgDsx* in *Blattella germanica*. RNAi of *BgTra*
984 in females generated a male-like body size and cuticle color, male-like tergal gland structure and a protruding

tissue at the end of the abdomen (left center); RNAi of *BgDsx* in males generated a female-like body color and a protruding tissue at the end of the abdomen, and the tergal gland partly disappeared (right bottom). Other treatments did not generate obvious developmental effects.

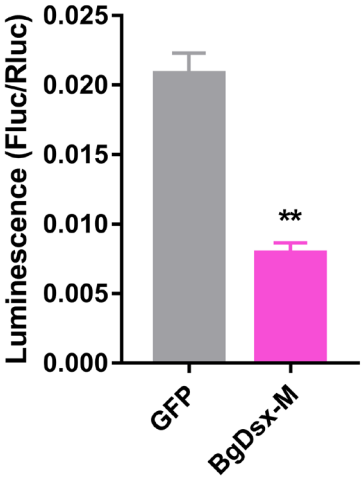

S9 Fig. Transcriptional activity of *BgDsx*^{M} on the upstream regulatory sequence of *BgElo12*. Data are shown as mean ± SEM; *P* values were calculated from 12 replicates; two-tailed Student's *t*-test.

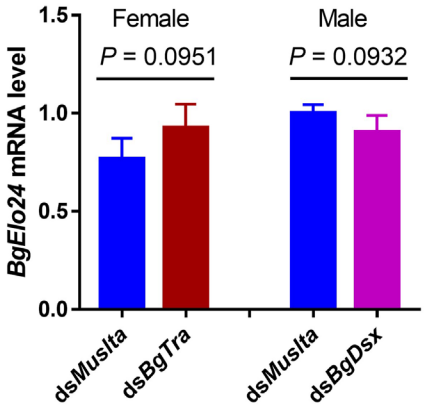

S10 Fig. Effects of *BgDsx*-RNAi in males and *BgTra*-RNAi in females on *BgElo24* expression. Data are shown as mean ± SEM; *P* values were calculated from 4 replicates (2 cockroaches/replicate); two-tailed Student's *t*-test.

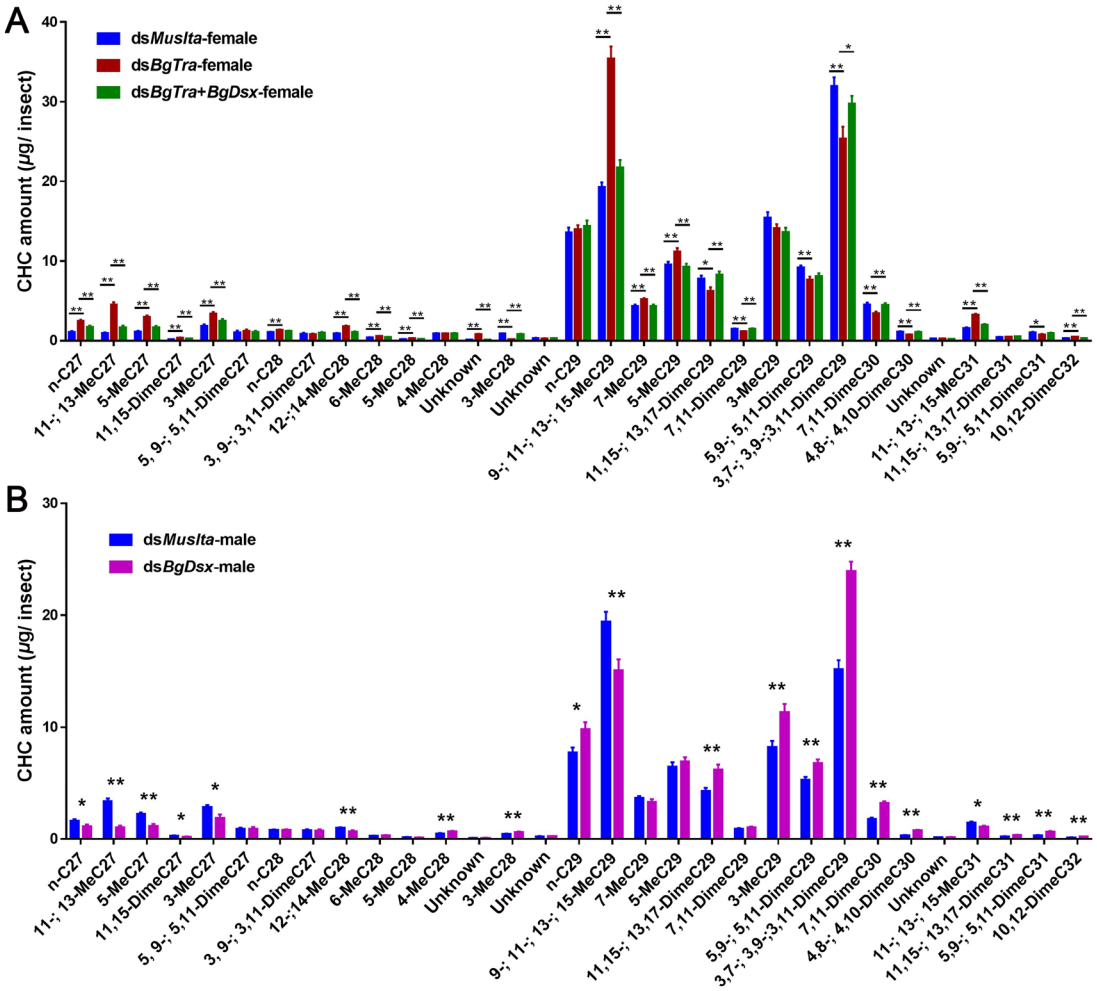

S11 Fig. Regulation of cuticular hrdrocarbon profiles by sex-differentiation genes. Data are shown as mean ± SEM, **P* < 0.05, ***P* < 0.01, two-tailed Student's *t*-test, n = 14 (ds*Muslta*-female), 12 (ds*BgTra*-female), 14 (ds*BgTra*+ds*BgDsx*-female), 12 (ds*Muslta*-male), and 16 (ds*BgDsx*-male).

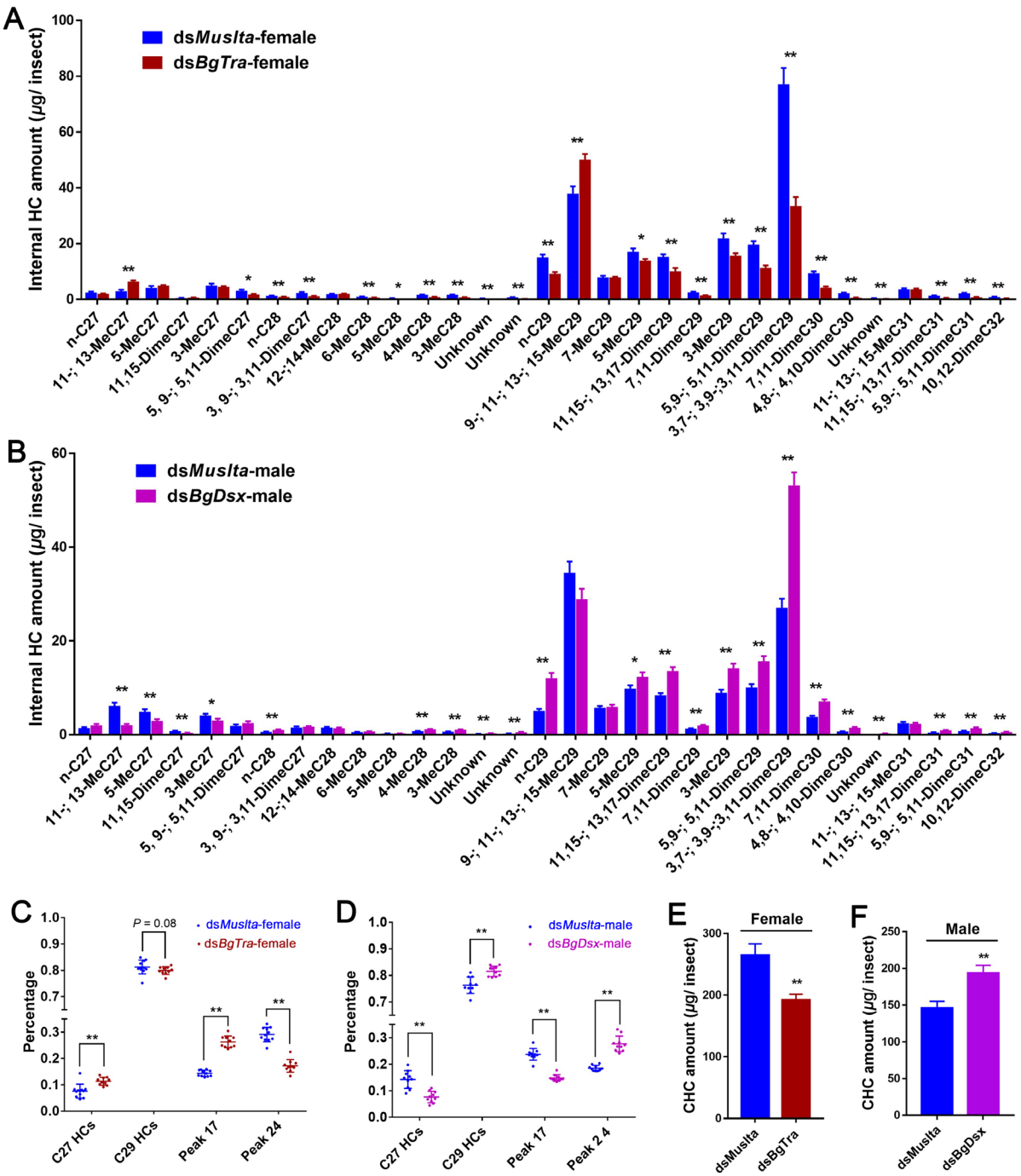

S12 Fig. Regulation of internal hrdrocarbon profiles by sex-differentiation genes. **(A)** and **(B)** Effects of *BgTra*-RNAi in females and *BgDsx*-RNAi in males on sex-specific internal hydrocarbon profiles. **(C)** and **(D)** Proportion changes of representative internal hydrocarbons after RNAi of *BgTra* in females and *BgDsx* in males. **(E)** and **(F)** Effects of *BgTra*-RNAi in females and *BgDsx*-RNAi in males on total amounts of internal hydrocarbons. Data are shown as mean ± SEM, **P* < 0.05, ***P* < 0.01, two-tailed Student's *t*-test, n = 10 or 11.

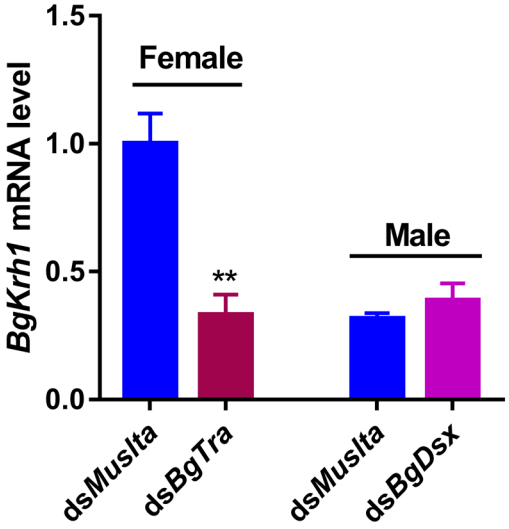

S13 Fig. Regulation of *BgKrh1* by *BgTra* in females. Data are shown as mean ± SEM, *P* values were calculated from 4 replicates (2 cockroaches/replicate), $^{**}P < 0.01$, two-tailed Student's *t*-test.

S1 Table. Quantification of difference cuticular hydrocarbons during sexual dimorphic cuticular hydrocarbons generation

S2 Table. Quantification of individual cuticular hydrocarbon after RNAi of other BgElo genes

S3 Table. Calculation the proportions of different fatty acid methyl esters in yeast expression

S4 Table. Primer sequences used in this study

S1 Appendix. Sequence alignment and protein structure analysis of BgElos